Annals of Mathematics **182** (2015), 491–564
http://dx.doi.org/10.4007/annals.2015.182.2.3

A polynomial upper bound on Reidemeister moves

By Marc Lackenby

Abstract

We prove that any diagram of the unknot with c crossings may be reduced to the trivial diagram using at most $(236\,c)^{11}$ Reidemeister moves.

1. Introduction

Turing stated in one of his famous articles [24] that '*No systematic method is yet known by which one can tell whether two knots are the same.*' Even the basic case of recognising the unknot is not obviously soluble. A few years later, in his groundbreaking work on normal surfaces, Haken solved the problem of recognising the unknot [11] and then made a crucial contribution to the more general problem of whether two knots are equivalent [12]. This was finally solved by the efforts of several mathematicians, including Hemion [17] and Matveev [22]. But it remains a major unresolved question to determine exactly how complex these problems are. The current state of our knowledge is that unknot recognition is in NP and co-NP. The fact that it is in NP is due to Hass, Lagarias and Pippenger [14] and that it is in co-NP was proved by Agol [1], but not written down in detail, and an alternative solution was given by Kuperberg [21], assuming the Generalised Riemann Hypothesis.

There are many examples of challenging diagrams of unknots. In 1934, Goeritz gave an example of a diagram with 11 crossings, with the property that any sequence of Reidemeister moves taking it to the trivial diagram must go via a diagram with more than 11 crossings. Other tricky examples have been given by Thistlethwaite, Haken, Henrich and Kauffman [18]. We include some of these in Figures 1–3. They all point to the probable conclusion that there is no simple way of recognising the unknot.

The most elementary and natural way of approaching the unknot recognition problem is to try to find an explicit upper bound on the number of Reidemeister moves required to turn a given diagram of the unknot with c crossings into the trivial diagram. It is easy to see that the existence of a computable

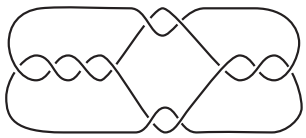

Figure 1. Goeritz's unknot

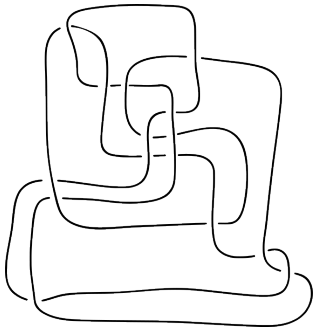

Figure 2. Thistlethwaite's unknot

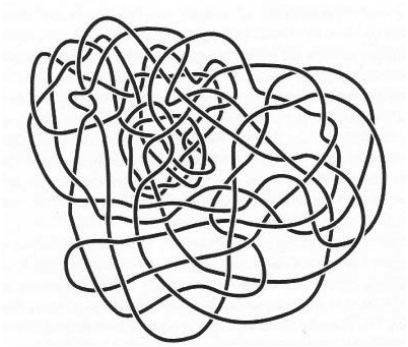

Figure 3. One of Haken's unknots (image courtesy of Cameron Gordon)

upper bound is equivalent to the solvability of the unknot recognition problem. But of course one wants a bound that is as small a function of c as possible.

In [13], Hass and Lagarias showed that a diagram of the unknot with c crossings can be converted into the trivial diagram using at most 2^{kc} Reidemeister moves, where $k = 10^{11}$. In [15], Hass and Nowik proved that, in general, at least $c^2/25$ moves are required. There is a large gap between these upper and lower bounds, and so it has remained a basic question: is there a polynomial upper bound on the number of Reidemeister moves required to turn an unknot diagram into the trivial diagram? This is what we solve in this paper.

THEOREM 1.1. *Let D be a diagram of the unknot with c crossings. Then there is a sequence of at most $(236\,c)^{11}$ Reidemeister moves that transforms D into the trivial diagram. Moreover, every diagram in this sequence has at most $(7\,c)^2$ crossings.*

It is worth pointing out that this does not actually improve our knowledge of the complexity class of the unknot recognition problem. But it does give an alternative way of establishing that the unknot recognition problem is in NP, because the sequence of Reidemeister moves provided by the above theorem gives a polynomial time certificate of unknottedness. Therefore, it remains an unsolved problem whether unknot recognition is in P. Of course, this may be very difficult, because a negative answer would imply that P $\neq$ NP. Moreover, it is unlikely that a polynomial time algorithm could be ruled out, even conditional upon the hypothesis that P $\neq$ NP, because it is widely conjectured that problems in NP $\cap$ co-NP are not NP-complete (see [10, p. 95]).

We also have a result for split links.

THEOREM 1.2. *Let D be a diagram of a split link with c crossings. Then there is a sequence of at most $(49\,c)^{11}$ Reidemeister moves that transforms D into a disconnected diagram. Moreover, every diagram in this sequence has at most $9\,c^2$ crossings.*

Our theorems rely in a crucial way on groundbreaking work of Dynnikov [8]. He considered a special way of arranging a knot or link called an arc presentation. One way of visualising these is via rectangular diagrams (also called grid diagrams), which are diagrams in the plane consisting of horizontal and vertical arcs, subject to the condition that the vertical arc always passes over the horizontal one at a crossing and the condition that no two arcs are collinear. The number of vertical arcs equals the number of horizontal arcs, and this is known as the *arc index* of this presentation. Dynnikov proved the surprising result that any arc presentation of the unknot can be reduced to the trivial presentation using a sequence of moves, known as exchange moves, cyclic permutations and destabilisations (see Figures 5–7). Crucially, the arc index never needs to increase. This has the striking consequence that if a diagram of the unknot has c crossings, then there is a sequence of Reidemeister moves taking it to the trivial diagram, such that all diagrams in this sequence have at most $2(c+1)^2$ crossings ([8, Th. 2]). But this does not give a polynomial upper bound on the number of such moves.

It is also possible to show that the approach of Hass and Lagarias in [13] does not provide a polynomial upper bound. They start with a diagram of the unknot with c crossings, and they use this to build a triangulation of a convex polyhedron with $t \leq 840c$ tetrahedra, each of which is straight in

$\mathbb{R}^3$ and which contains the given unknot in its 1-skeleton. From this, they construct a triangulation of the knot exterior. By work of Haken [11], the disc that the unknot spans can be realised as a normal surface with respect to this triangulation, and Hass and Lagarias show that at most 2^{kt} normal triangles and squares are required, where $k = 10^7$. They then isotope the unknot across this disc. The projection to the plane of the diagram then gives a sequence of Reidemeister moves. The bound on the number of normal squares and triangles gives the exponential bound on the number of Reidemeister moves. It does not seem feasible to use this approach of sliding the knot across a normal spanning disc to obtain a better bound on Reidemeister moves. This is because Hass, Snoeyink and Thurston [16] gave examples of unknots consisting of $10n + 9$ straight arcs, for which any piecewise linear spanning disc must have at least 2^{n-1} triangular faces.

Instead, our approach here is to combine Dynnikov's methods with the use of normal surfaces. Given an arc presentation for an unknot, Dynnikov explains how a spanning disc may be placed in what he calls admissible form. He defines a measure of complexity on such surfaces. The key part of his argument is to show that an admissible spanning disc must have at some point a certain local configuration. This then specifies a way of modifying the surface and the arc presentation. This has the effect of performing 'generalised exchange moves' on the arc presentation and possibly destabilisations. He shows that, during this process, either a destabilisation is performed or the complexity of the spanning disc has gone down.

Dynnikov defines a triangulation of the 3-sphere associated to an arc presentation of a link. If the arc index is n, this has n^2 tetrahedra. It turns out that placing the spanning disc or splitting sphere in admissible form is almost equivalent to placing this surface into normal form with respect to this triangulation. Moreover, his measure of complexity is (under reasonable assumptions) just the number of intersections between the disc or sphere and certain edges of the triangulation. Thus, using the bound on the complexity of normal surfaces that was proved by Hass and Lagarias in [13], the complexity of a splitting sphere is at most $n2^{7n^2}$. (A similar, but slightly larger, bound is required for the spanning disc of the unknot.) Hence, using Dynnikov's argument, one can show that the number of generalised exchange moves that one needs to perform before one can apply a destabilisation is at most an exponential function of n^2.

However, this is much larger than a polynomial upper bound. To obtain this, one needs to go deeper into normal surface theory. In a triangulated 3-manifold with n^2 tetrahedra, any normal surface consists of at most $5n^2$ types of normal triangles and squares. One can show that if there is a local configuration of the spanning disc or splitting sphere that specifies a way of reducing complexity, then one can also reduce complexity in regions of the

surface that are normally parallel. Thus, one might hope that, using a single generalised exchange move, one can reduce complexity by a factor of roughly $(1 - n^{-2})$. This is probably too optimistic, for it may be the case that most of the weight of the normal surface is concentrated in regions where this good configuration does not occur. The key technical part of this paper is to show that, under this situation, the surface does not have minimal complexity. In particular, there is another spanning disc or splitting sphere, with smaller complexity, for the same arc presentation. This is shown by establishing that some multiple of the given surface is actually a normal sum of a normal torus and a multiple of some simpler spanning disc or splitting sphere. The proof of this is somewhat delicate and relies on the use of branched surfaces and 'first-return maps.'

Thus, the results that we actually prove are as follows. (For the definitions of trivial and disconnected arc presentations, see Section 2.1.)

THEOREM 1.3. *Let D be an arc presentation of the unknot with arc index n. Suppose that the associated rectangular diagram has writhe k. Then there is a sequence of at most $4 \times 10^{18}\, n^{10}$ exchange moves, at most $6 \times 10^{18}\, n^9$ cyclic permutations, at most $10^{19}\, n^8$ generalised exchange moves, at most $3 \times 10^{13}\, n^6$ stabilisations and at most $3 \times 10^{13} n^6$ destabilisations taking D to the trivial arc presentation. Moreover, the arc index is at most $2n + |k| + 1$ throughout this sequence of moves.*

THEOREM 1.4. *Let D be an arc presentation of a split link with arc index n. Then there is a sequence of at most $3 \times 10^{11}\, n^8$ generalised exchange moves, at most $2 \times 10^{11}\, n^9$ cyclic permutations and at most $8 \times 10^{10}\, n^{10}$ exchange moves that takes D to a disconnected arc presentation.*

Now each generalised exchange move on an arc presentation with arc index n can be expressed as a composition of at most $(3/2)n^3$ Reidemeister moves (Lemma 2.4). Any exchange move is a product of at most n Reidemeister moves (Lemma 2.2). A cyclic permutation requires at most $(n-1)^2$ Reidemeister moves (Lemma 2.3). Also, given any diagram of a knot or link with c crossings, this is isotopic to a rectangular diagram with arc index at most $(81/20)c$ (Lemma 2.1). Any rectangular diagram with arc index n has at most $(n-1)^2/2$ crossings. (See the proof of Theorem 2 in [8].) These observations, combined with Theorems 1.3 and 1.4, imply Theorems 1.1 and 1.2.

The plan of the paper is as follows. In Section 2, we give some elementary properties of arc presentations. Section 3 contains an overview of Dynnikov's proof that arc presentations of the unknot and split links can be simplified using a sequence of exchange moves, cyclic permutations and destabilisations. In Section 4, we present an alternative argument, which provides an explicit upper

bound on the number of exchange moves, cyclic permutations, stabilisations and destabilisations required to trivialise a rectangular diagram of the unknot, given an upper bound for the complexity of the spanning disc. This is an unsurprising result and is required only in the case of the unknot. In Section 5, we recall some key facts from normal surface theory, including some results about vertex normal surfaces. We introduce a new notion of a boundary-vertex normal surface, which is useful in the parts of the proof dealing with the unknot. In Section 6, we introduce normal surface theory to arc presentations. We give Dynnikov's triangulation of the 3-sphere and explain how surfaces that are normal with respect to this triangulation have a form that is very close to admissible. Section 7 contains the proof of Theorems 1.3 and 1.4, assuming the result that the normal spanning disc or splitting sphere cannot contain large 'Euclidean' regions. This is proved in Sections 8 and 9, using branched surfaces. In the final section, we discuss possible improvements to the degree of the polynomial bound, and we also give some potential directions for further research.

The presence of surfaces with boundary causes several complications in these arguments, and so the case of the unknot is more complex than the case of split links. We therefore suggest that the reader initially concentrate on the split link case.

I would like to thank the referees for their very careful reading of an earlier version of this paper.

2. **Basic properties of arc presentations**

In this section, we present some elementary material on arc presentations and rectangular diagrams. Much of this was first discovered by Cromwell [6]. We have largely followed Dynnikov's presentation in [8].

2.1. *Definition of arc presentations.* We fix a description of the 3-sphere as the join $S^1 * S^1$ of two circles. The co-ordinate system (ϕ, τ, θ) is used, where $\phi, \theta \in \mathbb{R}/2\pi\mathbb{Z}$ are co-ordinates on the circles and $\tau \in [0,1]$. Thus, $(\phi, 0, \theta_1)$ and $(\phi, 0, \theta_2)$ are identified for all θ_1 and θ_2. Similarly, $(\phi_1, 1, \theta)$ and $(\phi_2, 1, \theta)$ are identified for all ϕ_1 and ϕ_2. The circles $\tau = 0$ and 1 are denoted by S^1_ϕ and S^1_θ respectively. The circle S^1_ϕ is called the *binding circle*. The open disc defined by $\theta = t$ and $\tau > 0$ is called a *page* and denoted $\mathcal{D}_t$.

Suppose that a link L satisfies the following two conditions: $L \cap S^1_\phi$ is a finite set, called the *vertices* of L, and for any $t \in \mathbb{R}/2\pi\mathbb{Z}$, the intersection $\mathcal{D}_t \cap L$ is either empty or an open arc approaching two distinct vertices. This is called an *arc presentation* of L. The number of vertices equals the number of pages that contain open arcs of L. This number is called the *arc index* of the arc presentation.

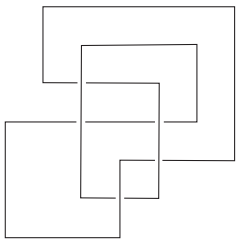

Figure 4. A rectangular diagram

We say that an arc presentation is *trivial* if it has arc index 2. We say that it is *disconnected* if there is a 2-sphere that intersects each page in a single embedded arc and that has components of L on both sides of it.

2.2. *Rectangular diagrams.* There is an equivalence between arc presentations and rectangular diagrams, which we now describe.

A *rectangular diagram* of a link L is a link diagram defined as follows. The plane of the diagram has a product structure $\mathbb{R} \times \mathbb{R}$. We require that the projection of L is a union of arcs, each of which is of the form $\{s\} \times [t_1, t_2]$ or $[s_1, s_2] \times \{t\}$. These are known as *vertical* and *horizontal arcs*. Whenever the interiors of two arcs of the projection intersect, the over-arc at the resulting crossing is required to be the vertical arc. Also, no two arcs may be collinear.

An arc presentation of L determines a rectangular diagram as follows. The arc presentation can be specified by the following data: the ϕ-values of the vertices, the values of θ where the page contains an arc, and the vertices at the endpoint of this arc. Let $s_1, \dots, s_n \in [0, 2\pi)$ denote the ϕ-values of the vertices, and let $t_1, \dots, t_n \in [0, 2\pi)$ denote the θ-values of the arcs. For each arc of L, lying in $\mathcal{D}_t$, joining vertices s_i and s_j where $s_i < s_j$, we insert a horizontal edge of the rectangular diagram at $[s_i, s_j] \times \{t\}$. For each vertex s of L, its two adjacent arcs lie in $\mathcal{D}_{t_i}$ and $\mathcal{D}_{t_j}$, where $t_i < t_j$. For each such vertex, we insert a vertical edge of the rectangular diagram at $\{s\} \times [t_i, t_j]$.

We now explain briefly why this is indeed a diagram of L. In fact, we will give a reasonably explicit map from the complement of the link defined by the arc presentation to the complement of the link defined by the rectangular diagram. (A more complete explanation is given in [6].)

Consider an arc presentation for L. We replace each arc of L in a page $\mathcal{D}_t$, joining vertices s_1 and s_2, where $s_1 < s_2$, by the concatenation of three arcs:

$$\begin{aligned} &\{\phi = s_1, \theta = t, \varepsilon \le \tau \le 1 - \varepsilon\} \\ \cup\, &\{s_1 \le \phi \le s_2, \theta = t, \tau = 1 - \varepsilon\} \\ \cup\, &\{\phi = s_2, \theta = t, \varepsilon \le \tau \le 1 - \varepsilon\}. \end{aligned}$$

Here, ε is some fixed real number in the interval $(0, 1/2)$. As L approaches a vertex s in pages $\mathcal{D}_{t_1}$ and $\mathcal{D}_{t_2}$, where $t_1 < t_2$, we replace it by an arc

$$\{\phi = s, t_1 \leq \theta \leq t_2, \tau = \varepsilon\}.$$

After this, L lies in the region $\{\varepsilon \leq \tau \leq 1 - \varepsilon\}$, which is a thickened torus. If we project onto $\{\tau = 1/2\}$, we obtain a diagram in a torus, and this torus is standardly embedded in S^3. Because we ensured that the arcs did not go beyond $\phi = 0$ and $\theta = 0$, the diagram lies in the square

$$\{0 \leq \phi < 2\pi, 0 \leq \theta < 2\pi, \tau = 1/2\}.$$

If we realise this square as a subset of the plane, we obtain the required rectangular diagram for L.

2.3. *From ordinary diagrams to rectangular diagrams.* Cromwell [6] proved that any link L has an arc presentation, by starting with an arbitrary diagram of L and making it rectangular. In this subsection, we will carry out this procedure, but we also keep track of an upper bound on the arc index of the resulting rectangular diagram.

LEMMA 2.1. *Let D be a diagram of a link with c crossings. Then D is isotopic to a rectangular diagram with arc index at most $(81/20)c$.*

Proof. We may clearly assume that D is connected. We may also assume that D contains no edge loops (which are arcs of the diagram with both endpoints at the same crossing). For we may remove all such edge loops, then isotope the resulting diagram so that it is rectangular, and then add back in the loops in a rectangular fashion.

Let X be the underlying 4-valent planar graph specified by D. This has $2c$ edges. We will modify X by subdividing its edges. If any pairs of edges are parallel, subdivide one of the edges from each pair. We may assume that at least six edges of the diagram are not parallel to any other edge, since otherwise D is a standard diagram of a $(2, n)$-torus link or a simple type of 2-bridge link, in which case the lemma is easy to establish. We deduce that X now has at most $2c + (2c - 6)/2 = 3c - 3$ edges.

In [23], Storer examined the problem of how to arrange a planar graph (with no edge loops or parallel edges) so that its edges are horizontal and vertical arcs, possibly after subdividing its edges. By Corollary 4 in [23], X may be subdivided so that it has a total of at most $(17/10)m + 4$ vertices, where m is the original number of edges of X, and then isotoped so that each edge is horizontal or vertical in the plane. So, the number of 2-valent vertices of X is now at most $(17/10)(3c - 3) + 4 - c \leq (41/10)c$.

This diagram might not be a rectangular diagram for two reasons. Firstly, some edges may be collinear. But if so, then a small modification, keeping the

arcs horizontal and vertical, can made to avoid this. Secondly, at some crossings, the over-arc may be horizontal, rather than vertical. But if so, there is an obvious modification that introduces eight new 2-valent vertices at such a crossing (see Figure 7 of [6]). Note that we may assume that at least half the crossings have the correct behaviour, as otherwise, we can instead just rotate the entire diagram by a quarter turn. So, the number of 2-valent vertices is at most $(41/10)c + 4c = (81/10)c$. The arc index of this rectangular diagram is at most half the number of 2-valent vertices, which is less than $(81/20)c$, as required. □

This bound of $(81/20)c$ is obviously not optimal. In fact, Cromwell and Nutt in [7] show that in many cases, the link specified by D has an arc presentation with arc index at most $c+2$. In the proof of Theorem 2 in [8], Dynnikov states that one can always find an arc presentation for the link with arc index at most $2c + 2$. However, the resulting rectangular diagram is not necessarily isotopic to D. So, to be able to use this fact in the proof of Theorems 1.1 and 1.2, one would need to be able to find an upper bound on the number of Reidemeister moves required to transform D into the new rectangular diagram. This is surely possible, but it is not completely straightforward. So, we have chosen to follow the simpler course of isotoping D so that it is rectangular, even though this might not lead to the optimal upper bound on arc index.

2.4. *Exchange moves, stabilisations and destabilisations.* Cromwell [6] introduced a set of moves that modify an arc presentation without changing the link. These are most simply visualised using rectangular diagrams:

(1) cyclic permutation of the horizontal (or vertical) arcs;
(2) stabilisation and destabilisation;
(3) interchanging parallel edges of the rectangular diagram, as long as they have no edges between them and their pairs of endpoints do not interleave; this is termed an *exchange move*.

These are shown in Figures 5–7.

When we use the term exchange move, we assume that the parallel edges that are moved past each other do not lie either side of $\theta = 0$ or $\phi = 0$. In this case, a cyclic permutation needs to be done first, before the exchange move can be performed. The reason we make this distinction is that an exchange move requires fewer Reidemeister moves in general than a cyclic permutation.

We now provide upper bounds on the number of these moves.

LEMMA 2.2. *Let n be the arc index of an arc presentation of L, and let D be the resulting rectangular diagram. Suppose that an exchange move is performed on this arc presentation, and let D' be the resulting rectangular diagram. Then D' and D differ by a sequence of at most n Reidemeister moves.*

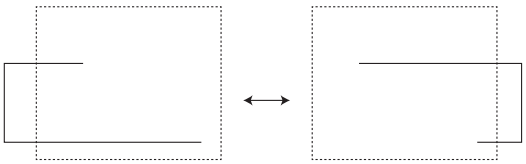

Figure 5. Cyclic permutation of the vertical edges

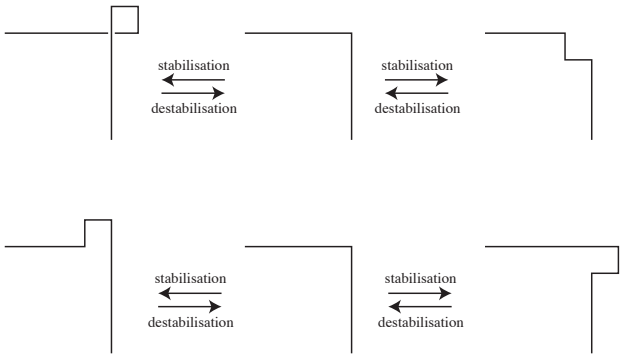

Figure 6. Stabilisations and destabilisations

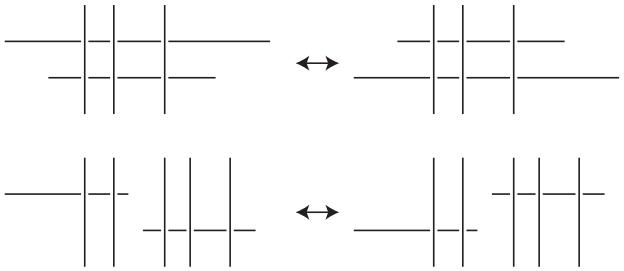

Figure 7. Exchange moves

Proof. This is fairly evident from Figure 7. In the bottom case of Figure 7, no Reidemeister moves are required. In the top case, one might first need to make a type 2 Reidemeister move to make the two horizontal edges overlap, then a sequence of at most $n-2$ type 3 Reidemeister moves, then possibly a type 2 move. □

LEMMA 2.3. *Let n be the arc index of an arc presentation of L. Suppose that a cyclic permutation is performed on the vertical (or horizontal) arcs. Then the resulting rectangular diagrams differ by a sequence of at most $(n-1)^2$ Reidemeister moves.*

Proof. In Figure 5, a vertical arc is slid across the diagram from left to right. As it meets another vertical arc, a type 2 Reidemeister move might need

to be performed, followed by a sequence of at most $(n-2)$ type 3 moves, then possibly a type 2 move if one was not performed at the beginning. This is at most $n-1$ Reidemeister moves. There are at most $n-1$ vertical arcs that it is slid across. So, at most $(n-1)^2$ Reidemeister moves are needed in total. □

2.5. *Generalised exchange moves.* A more substantial modification to an arc presentation was introduced in [6], known as a generalised exchange move. This is defined as follows.

Let $0 < s_1 < s_2 < s_3 < 2\pi$ be values of ϕ that are disjoint from the vertices of L. Let $0 \leq t_1 < t_2 < 2\pi$ be values of θ that are disjoint from the arcs of L. Suppose that each horizontal arc $[s, s'] \times \{t\}$ of the rectangular diagram satisfies the following conditions:

(1) if $t \in (t_1, t_2)$, then $\{s, s'\}$ is not interleaved with $\{s_2, s_3\}$;
(2) if $t \in S^1_\theta - (t_1, t_2)$, then $\{s, s'\}$ is not interleaved with $\{s_1, s_2\}$.

Then one can modify the rectangular diagram by changing the ϕ value of all the vertices between s_1 and s_2 so that they lie between s_2 and s_3 in the same order, and by changing the ϕ value of all the vertices between s_2 and s_3 so that they lie between s_1 and s_2 in the same order. This is a *generalised exchange move.*

The effect of a generalised exchange move on the rectangular diagram is shown in Figure 8, in the case where $t_1 = 0$, where it is evident that it does not change the link type.

LEMMA 2.4. *Let n be the arc index of an arc presentation of L. A generalised exchange move on this arc presentation is a composition of at most $(3/2)n^3$ Reidemeister moves. It is also a composition of at most n cyclic permutations and at most $(3/4)n^2$ exchange moves.*

Proof. In Figure 8, a generalised exchange move is shown where $t_1 = 0$. In general, as many as $n/2$ cyclic permutations may need to be made before $t_1 = 0$ and by Lemma 2.3, these may require at most $n^3/2$ Reidemeister moves.

Figure 8 shows how the generalised exchange moves can be divided into three steps. We estimate the number of Reidemeister moves or exchange moves required in the first step. Place each horizontal arc $[s, s'] \times \{t\}$ in one of the following sets:

(1) in A_1 if $s, s' \in (s_1, s_2)$ and $t \in S^1_\theta - (t_1, t_2)$;
(2) in A_2 if $s, s' \notin (s_1, s_2)$ and $t \in S^1_\theta - (t_1, t_2)$;
(3) in A_3 if $s, s' \notin (s_2, s_3)$ and $t \in (t_1, t_2)$;
(4) in A_4 if $s, s' \in (s_2, s_3)$ and $t \in (t_1, t_2)$.

So, the first step of the generalised exchange move slides the A_1 arcs past those in A_4 and some of those in A_2. It also slides the A_4 arcs past some of those in A_3. The number of exchange moves is therefore at most $|A_1||A_4| + |A_1||A_2| + |A_3||A_4| \leq (|A_1| + |A_3|)(|A_2| + |A_4|) \leq n^2/4$. The other two steps are

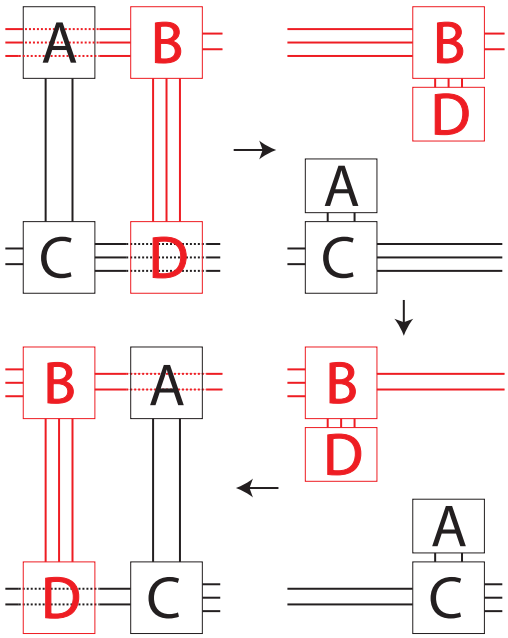

Figure 8. A generalised exchange move

similar, and so we obtain the required bound of $(3/4)n^2$ exchange moves. By Lemma 2.2, the first and third steps each require at most $n^3/4$ Reidemeister moves. The second step evidently needs no Reidemeister moves.

Finally, we reverse the cyclic permutations that were made initially. This is necessary because the generalised exchange move does not change the θ-value of any arc. Again, by Lemma 2.3, these require at most $n^3/2$ Reidemeister moves. So, in total, at most $(3/2)n^3$ Reidemeister moves are needed. □

2.6. *Generalised destabilisations.* Dynnikov also introduces another move called a *generalised destabilisation*. Here, one assumes that there are two arcs of L, one running from a vertex s_1 to a vertex s and the second running from s to a vertex s_2. Let the θ-values of these two arcs be t_1 and t_2. One assumes that there are no arcs of L with θ values in (t_1, t_2). Then, the generalised destabilisation replaces these two arcs of L by a single arc, running from s_1 to s_2, at height t_2, say.

In Figure 9, a generalised destabilisation is expressed as composition of exchange moves and a destabilisation. The following is clear.

Lemma 2.5. *Let n be the arc index of an arc presentation of L. Then a generalised destabilisation is the composition of at most n exchange moves, followed by a destabilisation.*

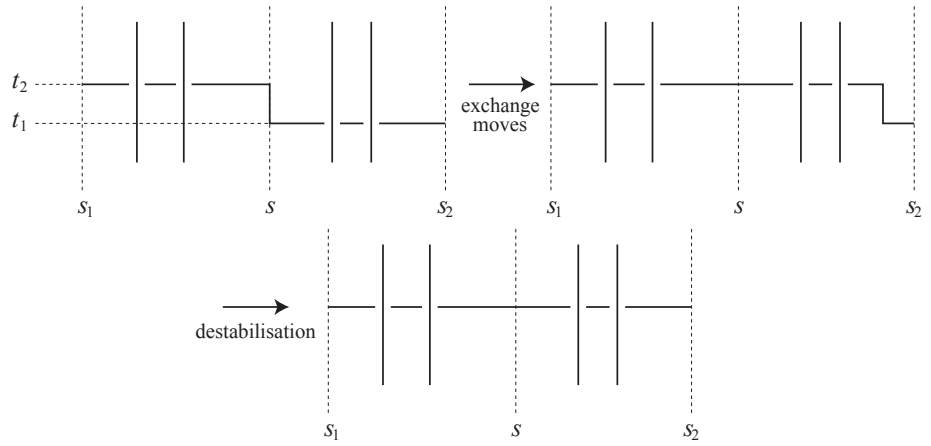

Figure 9. A generalised destabilisation

3. **A summary of Dynnikov's methods**

In this section, we give an overview of Dynnikov's work on monotonic simplification of arc presentations in [8]. This was highly influenced by Cromwell's initial investigations into arc presentations in [6]. In turn, this was influenced by the development of braid theory by Birman and Menasco (see [4] for example, or the survey in [3]) and Bennequin [2]. Our presentation in this section is substantially based on [8].

3.1. *Admissible form for characteristic surfaces.* When L is the unknot or a split link, there is an associated surface, which Dynnikov refers to as a *characteristic surface*. In the case of the unknot, this is a spanning disc. For a split link, it is a 2-sphere disjoint from the link, and with link components on both sides of it.

This surface S inherits a singular foliation $\mathcal{F}$ on $S - S^1_\phi$ defined by $d\theta = 0$. The intersection points $S \cap S^1_\phi$ are called the *vertices* of S.

Dynnikov places the characteristic surface S into *admissible form*, which is defined as follows:

(1) The surface S is smooth everywhere, except at $\partial S \cap S^1_\phi$.
(2) $S - \partial S$ intersects the binding circle S^1_ϕ transversely at finitely many points.
(3) The foliation $\mathcal{F}$ has only finitely many singularities, which are points of tangency of S with the pages $\mathcal{D}_t$.
(4) All singularities of $\mathcal{F}$ are of Morse type, i.e., local maxima, local minima or saddle critical points.
(5) Near any point of $(\partial S) \cap S^1_\phi$, the foliation $\mathcal{F}$ is radial.

(6) There is at most one point $p \in (\partial S) \cap S^1_\phi$ at which $|\int_\gamma d\theta| > 2\pi$, where $\gamma \subset S$ is a properly embedded arc in a small neighbourhood of p such that the endpoints of γ in ∂S lie on different sides of p. Such a point p is called a *winding vertex*. The quantity $|\int_\gamma d\theta|$ is the *winding angle* at this vertex.

(7) There is at most one point $p \in (\partial S) - S^1_\phi$ at which the surface S is not transverse to the corresponding page $\mathcal{D}_{\theta(p)}$. At the exceptional point, the foliation $\mathcal{F}$ must have a saddle critical point. If such a saddle and a winding vertex are both present, then the winding vertex is an endpoint of the edge containing the saddle.

(8) Each page $\mathcal{D}_t$ contains at most one arc of L and at most one singularity of $\mathcal{F}|_{S-\partial S}$, but not both.

Consider an arc of L, which is the intersection with some page, and suppose that it does not contain a saddle of S. Suppose that $\partial S = L$ (and so we are in the case where L is the unknot). Then, near this arc, except at the endpoints, all points of S satisfy one of the following:

(1) they have θ-values slightly greater than that of the arc, or
(2) they have θ-values slightly smaller than that of the arc.

We term this an *up* or *down* arc, respectively.

Now consider two incident arcs of L, neither of which contains a saddle of S. Then, by examining their common vertex, we see that one must be an up arc and one must be a down arc. So, as one travels along L, one meets up and down arcs alternately, with the possible exception of an arc containing a saddle. As a consequence, when the arc index of an unknot L is odd, then the characteristic surface must have a saddle somewhere on its boundary.

In the case where L is a split link, placing the characteristic 2-sphere into admissible form is a simple application of general position. However, when L is the unknot, a little more work is required. One first declares that the arcs of L are alternately up and down arcs, plus possibly one arc that contains a saddle of S. This controls the location of S near these arcs. Near each vertex of L, the foliation is required to be radial. When the vertex is not a winding vertex, this determines the behaviour of S near that vertex. At the winding vertex, the amount that the surface winds is chosen so that the curve $\partial N(L) \cap S$ has zero linking number with L. Thus, one first specifies the location of S near L, using this recipe. Then a small isotopy supported away from a small neighbourhood of L moves S into admissible form. More details can be found in the proof of Lemma 1 of [8].

3.2. *The structure of admissible surfaces.* Near a singular point of $\mathcal{F}$ or a vertex of S, there are the following possible local pictures:

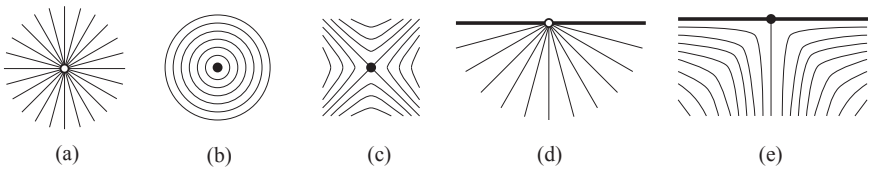

Figure 10. Singularities of the foliation

In (a), the behaviour near a point of $(S - \partial S) \cap S^1_\phi$ is shown. This is termed an *interior vertex* of $\mathcal{F}$. A *boundary vertex* is shown in (d), which is a point of intersection $\partial S \cap S^1_\phi$. The singularities shown in (b), (c) and (e) are called a *pole*, an *interior saddle* and a *boundary saddle*. We follow Dynnikov by denoting a vertex of S by a hollow dot and a Morse singularity by a solid dot.

When the singularities are removed from $\mathcal{F}$, the result is a genuine foliation on $S - S^1_\phi$. Each leaf is known as a *fibre*. (Dynnikov also calls the singularities of $\mathcal{F}$ fibres, but we do not do so here.) Therefore, fibres are of the following types:

(1) a closed circle,
(2) an open arc connecting two vertices,
(3) an open arc connecting a vertex to a saddle or a saddle to itself.

Note that an open arc cannot connect a vertex to itself, other than possibly a winding vertex. This is because the fibres emanating from a nonwinding vertex have distinct θ-values. Note also that a fibre cannot connect two distinct saddles, because each fibre lies in a single page and each page contains at most one saddle. A fibre that is incident to a saddle is termed a *separatrix*.

The complement of the vertices, the singular locus, the separatrices and the boundary of S has a special form. Each component of this complement we term a *tile*. This has a foliation induced by arcs and curves where θ is constant. It therefore admits a product structure. Hence, each tile is an open annulus or an open disc, which we term an *annular* and *disc* tile respectively. The discs have two vertices in their boundary, and at most two saddles. (When the boundary of a disc tile runs over fewer than two saddles, its closure contains an arc of L.) Note, however, that the boundary of a tile may run over the same saddle more than once, as shown in Figure 11. Hence, the closure of a disc or annular tile need not be a closed disc or annulus. There is a type of annular tile that is not shown in Figure 11, which has boundary consisting of just two vertices. In this case, S is a 2-sphere, and if it has components of L on both sides of it in S^3, then the arc presentation is disconnected. We may therefore assume that there are no such tiles.

Note that if there are any poles, then there are necessarily closed circle fibres near them. However, we will see shortly that poles can be readily removed. Closed circle fibres also arise near a separatrix that joins a saddle to

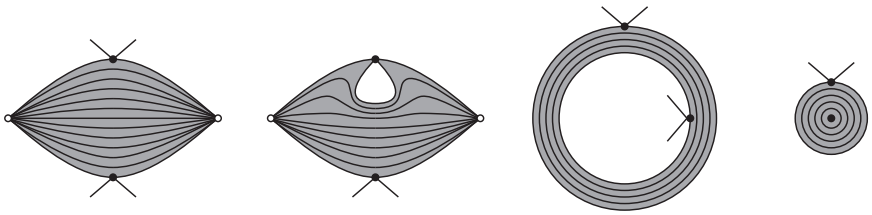

Figure 11. Some tiles

itself. Note, however, that in a small neighbourhood of each vertex of S, all the fibres are intervals.

Dynnikov defines the complexity of the characteristic surface S in admissible form to be the number of singularities of $\mathcal{F}$. We will use a slight variation of this. We will consider the *binding weight* $w_\beta(S)$, which is the number of intersections between S and the binding curve S^1_ϕ. In other words, the binding weight of S is the number of vertices of S, as shown in Figures 10(a) and 10(d).

3.3. *Reducing the complexity of the characteristic surface.* In [8], Dynnikov uses an Euler characteristic argument to show that the singular foliation $\mathcal{F}$ must contain certain configurations. In each case, he shows that one may either perform some exchange moves and cyclic permutations followed by a destabilisation, or one may perform some cyclic permutations, exchange moves and generalised exchange moves, after which one may reduce the complexity of the characteristic surface. There are eight possible configurations that he considers. However, in this paper, four of these play a particularly important role, and we will focus initially on these.

For a vertex s of $\mathcal{F}$, the closure of the union of all the fibres of $\mathcal{F}$ approaching s is called the *star* of s. The *valence* of s is the number of separatrices approaching s.

Dynnikov defines an interior vertex s as *bad* if one of the following cases arises:

(1) the star of s contains at least two fibres in distinct tiles that connect s to boundary vertices,
(2) the star of s contains a winding vertex.

If an interior vertex is not bad, it is *good*.

The main cases that we consider now are

(1) there is a pole,
(2) there is a good 2-valent interior vertex,
(3) there is a good 3-valent interior vertex,
(4) there is a 1-valent boundary vertex.

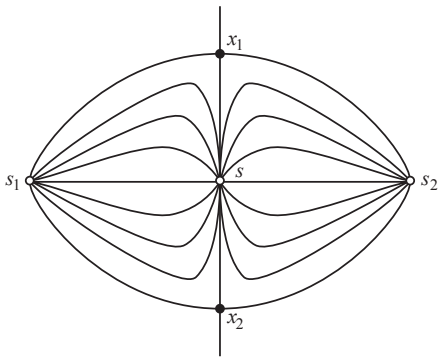

Figure 12. A good 2-valent vertex

These are not the only possible cases, but they are the only ones that we will be concerned with in this paper. Note that Dynnikov explains in the proof of Lemma 5 in [8] that there can be no 1-valent interior vertex.

3.4. *When there is a pole.* In this case, there is a simple modification that can be performed to the surface that reduces the number of singularities by 2 without changing the binding weight. One considers the tile incident to the pole. It has on its boundary a saddle. One can isotope the surface so as to cancel the pole and the saddle. This may move other parts of the surface, but it does not introduce any other singularities. The link itself does not need to be moved. In particular, no exchange moves, cyclic permutations or destabilisations are performed at this step.

3.5. *When there is a good* 2*-valent interior vertex.* Suppose that the characteristic surface S has a good 2-valent interior vertex s. Then Dynnikov shows that there is a generalised exchange move that can be applied to the arc presentation, which leaves the complexity of S unchanged, and then a further modification to the surface that reduces its complexity.

Adjacent to s, there are two disc tiles, and hence the configuration of $\mathcal{F}$ near s is as shown in Figure 12.

The resulting arrangement of the characteristic surface is shown in Figure 13. Dynnikov explains that, in this situation, one should perform a generalised exchange move, exchanging the intervals (s_1, s) and (s, s_2). This has the effect of modifying the foliation $\mathcal{F}$ without increasing its binding weight. One can then perform an isotopy to S, which reduces its binding weight by 2.

This procedure does not change the foliation near ∂S. In particular, no new winding vertices or boundary saddles are introduced. Moreover, in the case where L is the unknot, the decomposition of L into 'up' and 'down' arcs, plus possibly one extra arc, remains unchanged.

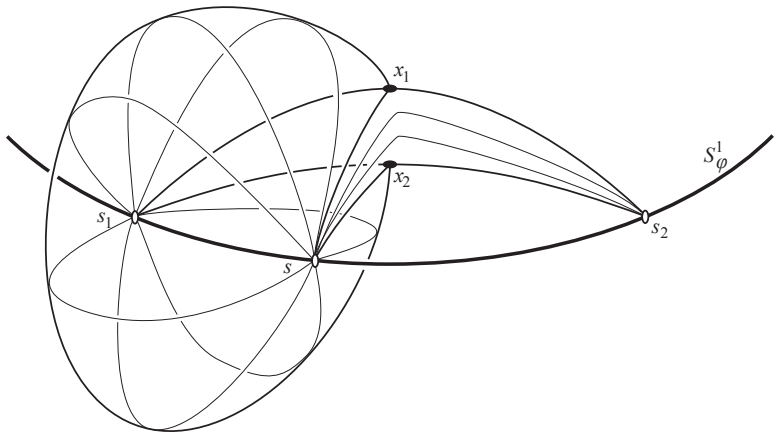

Figure 13. The arrangement of the characteristic surface

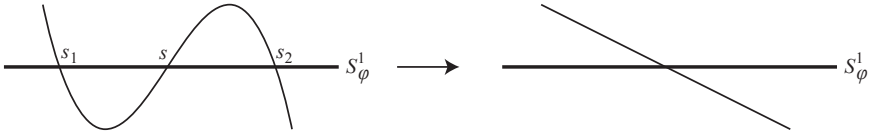

Figure 14. The ambient isotopy of S

3.6. *When there is a good* 3*-valent interior vertex.* When there is a good 3-valent interior vertex, Dynnikov explains how one can isotope S without increasing its binding weight to create a good 2-valent interior vertex. This is admirably described in the proof of Lemma 6 in [8], and so we only give a sketch here.

Let s be the good 3-valent interior vertex. Let s_2, s_3 and s_4 be the three vertices in its star. Without loss of generality, suppose that they are arranged around S^1_ϕ in the order s, s_2, s_3, s_4. Let x_1 be the saddle that is connected by separatrices to s, s_2 and s_3, and let s_5 be the other vertex connected to x_1 by a separatrix. Let x_2 be the saddle that is connected by separatrices to s, s_3 and s_4, and let s_6 be the other vertex connected to x_2 by a separatrix. A picture of the foliation near s is shown in the left of Figure 15. Let $t_1 = \theta(x_1)$ and $t_2 = \theta(x_2)$. Suppose, without loss of generality, that the fibres joining s and s_3 have θ values lying in the interval (t_1, t_2).

The first thing that one does is perform at most $n/2$ cyclic permutations, so that $0 < t_1 < t_2 < 2\pi$. Then Dynnikov explains that all events in the interval (t_1, t_2) need to moved out of this interval, where an *event* is the occurrence of a saddle or an arc of the link in some page $\mathcal{D}_t$, where $t \in (t_1, t_2)$. This is done by moving the events with endpoints in (s, s_3) into the future, so that they happen after t_2, and by moving the events with endpoints in (s_3, s) into the

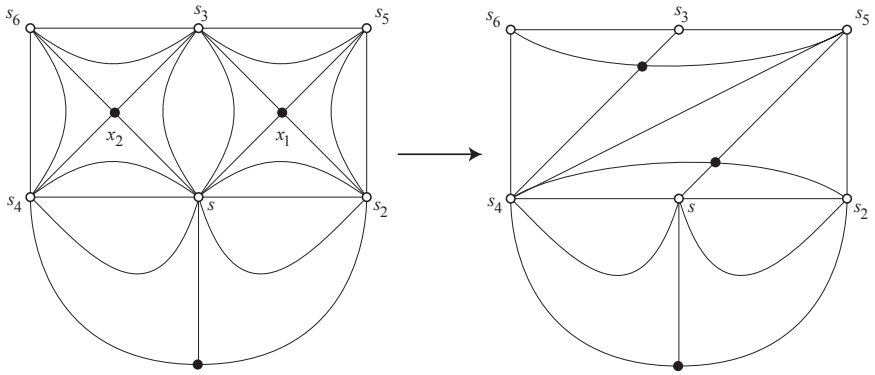

Figure 15. A good 3-valent vertex

past, so that they happen before t_1. In particular, the arcs of the link in these intervals need to be moved past each other using exchange moves. Suppose that there are m such arcs with endpoints in the interval (s, s_3). Then there are at most $n - m$ arcs with endpoints in the interval (s_3, s) that need to be moved. So at most $m(n - m) \leq n^2/4$ exchange moves are required.

Once this has been achieved, one then performs an isotopy, which has the effect on the foliation as shown in Figure 15. This turns s into a good 2-valent interior vertex, and so one then proceeds as in Section 3.5.

As in Section 3.5, this procedure does not change the foliation near ∂S.

3.7. *When there is a* 1*-valent boundary vertex.* In this case, there are two possibilities for the configuration of $\mathcal{F}$ near the 1-valent boundary vertex s. These depend on whether or not there is a boundary-saddle in the star of s. They are shown in Figure 16. In both cases, Dynnikov gives a modification to L and S. We concentrate on the case where the star of s does not contain a boundary saddle. The other case is similar.

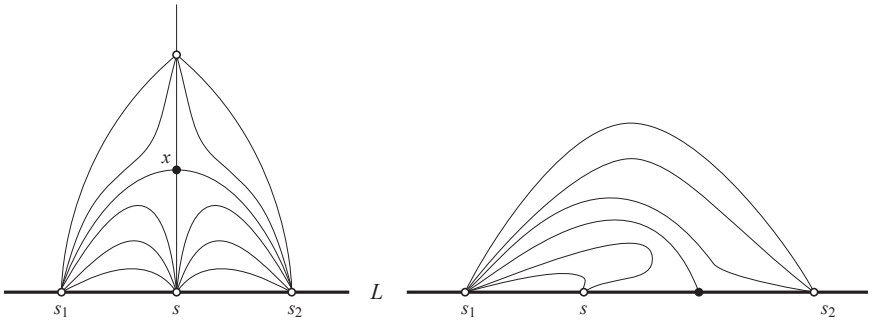

Figure 16. A 1-valent vertex s

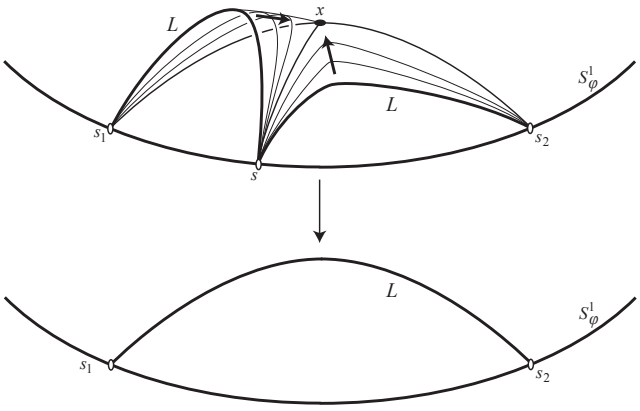

Figure 17. The ambient isotopy of S

Now, it cannot be the case that s and s_1 are both winding vertices, since S is admissible. Hence, the tile that is incident to both of them has total θ-angle less than 2π. There is therefore some page that is disjoint from this tile. We first perform at most $n/2$ cyclic permutations so that this page is at $\theta = 0$. We then slide the arc of L that joins s and s_1 across this tile, maintaining it in pages. This has the effect of performing some exchange moves. At most n of these are performed in total because the tile containing s and s_1 is disjoint from the page $\mathcal{D}_0$.

We now consider the tile containing s and s_2. We perform at most $n/2$ cyclic permutations so that the tile misses the page $\mathcal{D}_0$. Then we slide the arc of L that joins s and s_2 across this tile. This process is stopped when the two arcs of L have adjacent θ-values. Then a generalised destabilisation is performed. By Lemma 2.5, this is a composition of at most n exchange moves, followed by a destabilisation.

This procedure does not introduce any winding vertices, since the θ-angle around each of the vertices s_1 and s_2 is reduced. However, the resulting surface need not be in admissible form, because the saddle (labelled x in the left of Figure 16) becomes a boundary-saddle. If S already has a boundary-saddle elsewhere, then a further isotopy is necessary if one wants the resulting surface to be in admissible form. In the next section, we introduce a variation of admissible form, which we term alternative admissible form, which is partly designed to get around this complication.

4. **Simplifying arc presentations of the unknot**

In the previous section, we gave an outline of Dynnikov's argument, which provides a sequence of exchange moves, cyclic permutations and destabilisations taking an arc presentation of the unknot or split link to a trivial or

disconnected presentation. The argument relied on destabilising the arc presentation or reducing the binding weight of the characteristic surface at each stage. It is not very surprising that the number of moves that are required can be bounded in terms of the initial binding weight. In this section, we prove a result along these lines. The main complication is that it is not the case that, in Dynnikov's argument, a single exchange move is used to reduce the binding weight by one. Many moves may be needed, and these need to be quantified. It is possible to do this by carefully analysing Dynnikov's proof, but the resulting upper bound on the number of exchange moves and cyclic permutations is not optimal. Instead, we present a variant of Dynnikov's theorem and proof, which leads to a better bound. We are very grateful to Ivan Dynnikov for suggesting that a proof along these lines would be possible. This relies on a slightly modified version of admissible form, which is as follows.

Let L be a link with a given arc presentation. Let S be a compact surface embedded in S^3 with interior disjoint from L and with each component of ∂S being a component of L. Then S is in *alternative admissible form* if it satisfies (1), (2), (3), (4), (5) and (8) in the definition of an admissible surface, together with the following:

(9) there are no winding vertices,
(10) each arc of L contains at most one boundary saddle of S.

This has some advantages and some disadvantages over admissible form. The main disadvantage is that it might not be possible to isotope a given surface into alternative admissible form, keeping the link fixed. But it is possible to do so after stabilising.

LEMMA 4.1. *Let D be an arc presentation of the unknot L with arc index n. Let S be a spanning disc in admissible form. Suppose that it is not in alternative admissible form and hence has a winding vertex. Let its winding angle be at most $2\pi m$ for some positive integer m. Then, there is a sequence of $m-1$ stabilisations and at most $(m-1)(n+m)$ exchange moves, taking D to a new arc presentation D', after which we may isotope S to an alternative admissible surface, keeping L fixed. The difference between the binding weight of S' with respect to D' and the binding weight of S with respect to D is $m-1$.*

Proof. When a stabilisation is performed on an arc presentation, it occurs near a vertex s of L. A new arc of L is inserted into some page $\mathcal{D}_t$. If we then perform at most n exchange moves, we may take t to be any value, as long as this page contains no other arcs of L. We may also suppose that $\mathcal{D}_t$ contains no singularities of the given admissible surface S. If there is a fibre of the singular foliation on S that is incident to s and that lies in the page $\mathcal{D}_t$, then there is an obvious way of isotoping S so that, with respect to the new arc presentation, conditions (1), (2), (3), (4), (5), (6) and (8) in the definition of

admissibility hold. The effect of this on the singular foliation near s is shown in Figure 18. Away from this regular neighbourhood of s, the singular foliation is unchanged. We may do this $m-1$ times at the winding vertex of S, so that the resulting surface S' has no winding vertex. Note that each arc of L ends up with at most one boundary saddle. Hence, this surface is now in alternative admissible form. □

We can now give an upper bound on the number of moves required to trivialise an arc presentation of the unknot.

THEOREM 4.2. *Let D be an arc presentation for the unknot L with arc index n. Let S be a spanning disc that is in alternative admissible form, with binding weight $w_\beta(S)$. Then, there is a sequence of at most $4n^2 w_\beta(S)$ exchange moves, at most $n w_\beta(S)$ cyclic permutations, at most $w_\beta(S)$ stabilisations and at most $w_\beta(S)$ destabilisations that takes D to the trivial arc presentation. Moreover, throughout this sequence, the arc index remains at most $n+1$.*

Stabilisations are used here and in Lemma 4.1, and so this is not 'monotonic simplification' in the sense of Dynnikov [8].

Note that if $w_\beta(S)$ is bounded above by a polynomial function of the arc index n, then the number of moves given by Theorem 4.2 is also bounded above by a polynomial in n.

Proof. Because S is in alternative admissible form, it inherits a singular foliation. The language of admissible surfaces readily translates to this setting. However, we modify the definition of good and bad vertices, as follows. An interior vertex of S is now *bad* if its star contains fibres f_1 and f_2 in distinct tiles, both of which are incident to boundary vertices, and such that both components of $S \backslash \mathrm{cl}(f_1 \cup f_2)$ contain at least one vertex of S. We say that a boundary vertex is *bad* if its star contains a fibre f that is also incident to some other boundary vertex, and such that both components of $S \backslash \mathrm{cl}(f)$ contain at least one vertex of S. We say that a vertex is *good* if it is not bad.

We may assume that S has no poles, since if S contains a pole, then there is a simple modification to S that reduces its number of singularities without changing its binding weight and without moving L.

For a vertex s of S, define its *interior valence* $d_i(s)$ and *boundary valence* $d_b(s)$ to be the number of separatrices approaching s that lie in the interior of

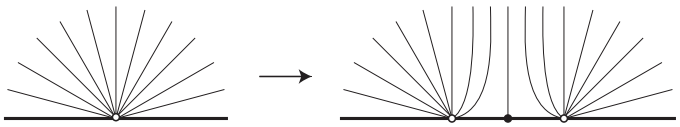

Figure 18. Stabilising near a vertex

S and the boundary of S respectively. So, the sum of these two quantities is the valence of s.

CLAIM. *There is either a good interior vertex with valence* 2 *or* 3, *or a good boundary vertex* s *such that* $2d_i(s) + d_b(s) \leq 3$.

In order to prove this, we will first construct a graph G embedded in S. For each bad interior vertex and for each tile in its star that is incident to a boundary vertex, pick a fibre in that tile and make it an edge of the graph. For each tile incident to two boundary vertices and that does not contain an arc of L in its closure, pick a fibre in that tile, which runs between these two vertices, and make it an edge of G. Take the vertices of G to be the endpoints of these edges.

This graph divides S into discs. We will now pick one of these discs, S', carefully. If G is empty, then set $S' = S$. So, suppose that G is nonempty. Let $N(G)$ be a thickening of G away from ∂S. This is almost a regular neighbourhood, except that $N(G) \cap \partial S = G \cap \partial S$. Let α be $\partial N(G)$. Thus, α is a union of properly embedded arcs, with disjoint interiors but which may intersect at their endpoints. Each arc of α runs parallel to one or two edges of G. We say that an arc α' of α is *trivial* if some component of $S \backslash \alpha'$ contains no vertices of S. In this case, the corresponding component of $S \backslash G$ contains a single separatrix running from a vertex of G to a boundary saddle. Let α_- be the result of removing all trivial arcs from α. Pick an arc of α_- that is outermost in the disc S. This separates off a disc S' with no arcs of α_- in its interior. Suppose first that S' is not disjoint from G. Then S' contains at least two trivial arcs of α, and so we deduce that S' contains a good boundary vertex s with $d_b(s) = 2$ and $d_i(s) = 0$, as required by the claim. Thus, we may assume that S' is disjoint from G. It therefore corresponds to a component of $S \backslash G$, which we will also call S'.

If G is nonempty, then $\mathrm{cl}(S') \cap G$ is either a single edge joining two bad boundary vertices or two edges joined at a bad interior vertex of S. Note that, by construction, S' contains at least one vertex of S that does not lie in G.

Now glue two copies of $\mathrm{cl}(S')$ along the two copies of $\mathrm{cl}(S') \cap \partial S$. Denote the resulting surface by S_+. It is either a disc or sphere. This surface S_+ has a singular foliation. It has either zero, two or four vertices in its boundary. In the latter case, at least one of these vertices has valence greater than one. For if all four vertices in ∂S_+ have valence 1, then it is easy to check that S' contains no vertices, which is impossible.

Note that S_+ has no boundary saddles. Let v_2^i and v_3^i be the number of interior vertices of S_+ with valence 2 and 3 respectively. Let v_1^b be the number of boundary vertices of S_+ with valence 1. Then $v_1^b < 4$. Using the fact that S_+ has positive Euler characteristic, Dynnikov's argument in the proof of Lemma

5 in [8] gives that $2v_2^i+v_3^i+v_1^b \geq 4$. (See formula (8) in [8] for example.) Hence, S_+ contains in its interior a vertex with valence at most 3. This came from a good vertex s of S. When s is in the interior of S, it is the vertex required by the claim. (Note that a vertex in the interior of S cannot have valence 1.) So, suppose that s lies in the boundary of S. Each separatrix in the star of s that lies in the interior of S gives rise to two separatrices in S_+. Each separatrix in the boundary of S gives rise to just one separatrix of S_+. So, we deduce that $2d_i(s) + d_b(s) \leq 3$, which proves the claim.

When there is a good interior vertex in S with valence 2 or 3, we would like to apply the procedure described in Sections 3.5 and 3.6. However, there is one minor complication. We have modified the definition of a good interior vertex, and so an interior vertex s that was bad with the previous definition may now be good. In the star of such a vertex s, there are two fibres f_1 and f_2 lying in distinct tiles, which are incident to boundary vertices s_1 and s_2, say, and such that one component of $S\backslash \mathrm{cl}(f_1 \cup f_2)$ contains no vertex of S. We are concerned with the situation where s has valence 2 or 3, and so we now consider these two cases.

Suppose first that s has valence 3. Then, the local picture near s may not be quite as shown in Figure 15. One or both of the saddles x_1 and x_2 may be boundary saddles, in which case the vertices s_5 or s_6 might not be present. If x_1 and x_2 are both boundary saddles, then we focus instead on s_3, which is a good boundary vertex with $d_b(s_3) = 2$ and $d_i(s_3) = 0$. Such vertices are dealt with later in the argument. So, we may suppose that at most one of x_1 and x_2 is a boundary saddle. If x_2 is a boundary saddle, the isotopy described in Section 3.6 may still be applied. When x_1 is a boundary saddle, we swap the roles of x_1 and x_2, and so when we apply the isotopy described in Section 3.6, the resulting foliation is the mirror image of that shown in the right in Figure 15 without the vertex s_5. Therefore, in both cases, the valence of s can be reduced to 2. It remains good.

So, suppose now that the valence of s is 2. If s is a good interior vertex that was bad using the previous definition, then the singular foliation near s is shown in Figure 19. The arrangement of the characteristic surface still is as shown in Figure 13, but now the arc in S running from s_1 to s_2 via x_1 is actually an arc of L. It is clear that the generalised exchange move and the isotopy of Figure 14 may still be applied, as along as they are combined with a generalised destabilisation of L that removes this arc.

These procedures reduce the binding weight by 2 and require at most n cyclic permutations, at most $n^2 + n$ exchange moves and at most one destabilisation.

We now consider the case where there is a good boundary vertex s such that $2d_i(s) + d_b(s) \leq 3$. Hence, we are in one of the following situations:

(1) $d_b(s) = 0$ and $d_i(s) = 0$,
(2) $d_b(s) = 0$ and $d_i(s) = 1$,
(3) $d_b(s) = 1$ and $d_i(s) = 0$,
(4) $d_b(s) = 1$ and $d_i(s) = 1$,
(5) $d_b(s) = 2$ and $d_i(s) = 0$.

Note that $d_b(s) \leq 2$, since at most two separatrices in the star of s lie in the boundary of S.

We may assume that Case (1) does not arise, because a vertex cannot have zero valence, unless the arc presentation is already is trivial.

Cases (2) and (3) are shown in Figure 16. As explained in Section 3.7, we may apply sequence of at most n cyclic permutations, at most $3n$ exchange moves and then a destabilisation. After this, the spanning surface remains in alternative admissible form. Its binding weight has been decreased by 1. Note that in Case (2), the saddle x that is in the star of the vertex becomes a boundary saddle in the new spanning surface. The fact that boundary saddles can be created in this way is one of the reasons why we use alternative admissible form.

In Cases (4) and (5), a new move is required. We will focus on Case (5), but Case (4) is similar. A picture of the star of s is shown in Figure 20. Note that s_1 lies in the interior of S, because s is good. We first perform

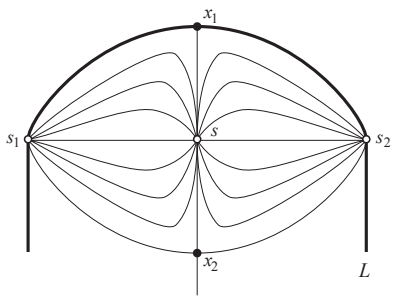

Figure 19. A 2-valent interior vertex that is now good

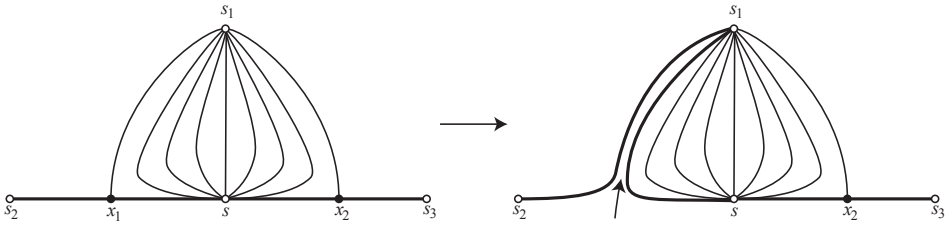

Figure 20. Case (5) in the proof of Theorem 4.2

a generalised stabilisation that replaces the arc of L between s and s_2 by two arcs, one running from s to s_1, the other running from s_1 to s_2. By Lemma 2.5, this is a composition of a stabilisation and at most n exchange moves. These new arcs of L follow fibres of the foliation of S that lie near the separatrices incident to x_1. The unknot L with this new arc presentation inherits a spanning disc, which is a subset of S, in alternative admissible form. This is shown in the right of Figure 20. With respect to this new surface, $d_b(s) = 1$ and $d_i(s) = 0$. So, we are in Case (3), and therefore a sequence of at most n cyclic permutations, at most $3n$ exchange moves and then a destabilisation can be performed. Note that, although a stabilisation has been performed, it is followed by a destabilisation, and so the arc index remains at most n after this process.

Since the binding weight has decreased by at least 1 at each stage, and we have bounded the number of exchange moves, cyclic permutations, stabilisations and destabilisations at each stage, the theorem follows immediately. □

5. **Normal surfaces**

In this section, we recall some key aspects of normal surface theory. We also extend the theory a little by introducing the new concept of a boundary-vertex normal surface.

5.1. *Definitions.* Let P be a compact 3-dimensional polyhedron. Then a disc properly embedded in P is said to be *an elementary normal disc* if

(1) it is disjoint from the vertices and intersects the edges transversely,
(2) it intersects each face in a collection of properly embedded arcs, and
(3) it intersects each edge at most once.

When P is a tetrahedron, an elementary normal disc necessarily intersects the 1-skeleton in three or four points. Normal discs of this form are called *triangles* and *squares*. Examples are shown in Figure 22.

Let M be a compact 3-manifold with a polyhedral decomposition $\mathcal{P}$. Then a surface properly embedded in M is *normal* if it intersects each polyhedron in a disjoint union of elementary normal discs.

Note that this is a variation on the usual notion of normality. Many authors require that elementary normal discs satisfy an extra condition: for each arc of intersection with an interior face, the endpoints of the arc do not lie on adjacent edges, one of which is in ∂M, while the other is not. We do not make this requirement here. Our notion of normality is very close to that used by Jaco and Oertel in [19].

We say that an arc properly embedded in a 2-dimensional polygon is *normal* if it is disjoint from the vertices and has endpoints in distinct edges. When M has a polyhedral decomposition, its boundary ∂M also inherits a

polyhedral structure. We say that a collection of disjoint simple closed curves in ∂M is *normal* if its intersection with each face in ∂M is a collection of normal arcs.

One of the key tenets of normal surface theory is that many topologically relevant surfaces may be placed in normal form. This is usually proved by showing that, when a properly embedded surface is not normal, then there is a modification that can be made to it that reduces the number of intersections with the 1-skeleton. Hence, a surface with minimal number of intersections with the 1-skeleton (among a suitable collection of surfaces) is typically normal. In fact, when the surface is closed, these modifications do not increase the number of intersections with any edge. (See Theorem 3.3.21 in [22] for example.) We may therefore obtain a version of this result that uses a variation of the usual notion of complexity, which is defined as follows.

Let M be a compact 3-manifold with a polyhedral decomposition $\mathcal{P}$. Fix a subcomplex β of the 1-skeleton. For a surface S properly embedded in M in general position with respect to the 1-skeleton of $\mathcal{P}$, define the *weight* of S, denoted $w(S)$, to be the number of intersection points between S and the 1-skeleton of $\mathcal{P}$. Define the *β-weight* of S to be the number of intersection points between S and β, denoted $w_\beta(S)$. We will consider the pair $(w_\beta(S), w(S))$ and order these pairs lexicographically. Thus, $(w_\beta(S), w(S))$ is less than $(w_\beta(S'), w(S'))$ if and only if *either* $w_\beta(S) < w_\beta(S')$, *or* $w_\beta(S) = w_\beta(S')$ and $w(S) < w(S')$.

Note that the terminology $w_\beta(S)$ is already being used to denote the binding weight of an admissible surface S. This is intentional, because later in the paper, we will choose $\mathcal{P}$ and β so that these quantities coincide.

A straightforward modification to the proof of Theorem 3.3.21 in [22] gives the following result.

THEOREM 5.1. *Let M be a compact orientable 3-manifold with a polyhedral decomposition $\mathcal{P}$ that has a subcomplex β in its 1-skeleton. Suppose that M is reducible. Then there is a reducing sphere S in normal form, such that $(w_\beta(S), w(S))$ is minimal among all reducing spheres that are in general position with respect to the 1-skeleton.*

We will also need to work with normal surfaces with boundary. In this case, the usual normalisation procedure may need to move the boundary of a surface. With the strong notion of normality that is used by many authors, this movement of the boundary of the surface is hard to avoid. However, with the weaker version of normality we are using in this paper, it is possible to ensure that the boundary of the surface does not need to be moved, under a fairly mild hypothesis. The main modification occurs when there is an arc of intersection between the surface S and an interior face of the polyhedral

decomposition with endpoints on the same edge and with this edge lying in ∂M. Then, usually one performs a boundary compression to simplify the surface. If S is orientable, then its boundary inherits an orientation and we see that, in this situation, the boundary of the surface intersects this edge in two points of opposite sign. Thus, if we ensure that this does not arise, then this modification is not required. We therefore obtain the following result.

THEOREM 5.2. *Let M be a compact orientable 3-manifold with a polyhedral decomposition $\mathcal{P}$ that has a subcomplex β in its 1-skeleton. Suppose that M has compressible boundary. Let C be a normal simple closed curve in ∂M that bounds a disc in M. Suppose that, for each edge in ∂M, all points of intersection between C and that edge have the same sign. Then there is a compression disc S in normal form, with $\partial S = C$, such that $(w_\beta(S), w(S))$ is minimal among all compression discs that are in general position with respect to the 1-skeleton and that have boundary equal to C.*

5.2. *The normal surface equations.* Let M be a compact 3-manifold with a polyhedral decomposition $\mathcal{P}$. Suppose that there are k types of elementary normal discs in $\mathcal{P}$. Then each properly embedded normal surface S in M determines a sequence of nonnegative integers $(x_1, \dots, x_k)$. Each x_i is the number of elementary normal discs of a fixed type and is called the *co-ordinate* of this disc type. This sequence is known as the *normal surface vector* for S, and we denote it by $[S]$.

This vector satisfies a system of linear equations called the *matching equations*. There is a set of equations for each face F of $\mathcal{P}$ with polyhedra on both sides. When S is a normal surface properly embedded in M, the elementary discs in the polyhedra adjacent to F intersect F in a collection of normal arcs. For each type of normal arc in F, there must be the same number of arcs of this type from the polyhedra on both sides. These conditions are the matching equations.

Some elementary normal disc types in a polyhedron necessarily intersect. We call two discs of this type *incompatible*. Thus, incompatible elementary discs cannot occur in a properly embedded normal surface. For example, in the case of a tetrahedron, two squares of different types necessarily intersect. Therefore the vector for a normal surface satisfies the constraints that, for each pair of incompatible disc types, force the co-ordinate of at least one of them to be zero. These conditions are called the *compatibility conditions*.

The following key result is one of the cornerstones of normal surface theory (for example, see [19, §1]).

THEOREM 5.3. *There is a one-one correspondence between properly embedded normal surfaces, up to normal isotopy, and solutions to the matching equations by nonnegative integers that satisfy the compatibility conditions.*

Because of this strong relationship between normal surfaces and solutions to certain equations, it is useful to take advantage of tools from linear algebra.

The *normal surface solution space* $\mathcal{N}$ is the set of vectors in $\mathbb{R}^k$ with non-negative *real* co-ordinates that satisfy the matching equations and the compatibility conditions. Thus, the points of $\mathcal{N} \cap \mathbb{Z}^k$ correspond to properly embedded normal surfaces.

It is easy to see that the normal surface solution space has a polyhedral structure in the sense that it is a union of convex polytopes glued along certain faces. More specifically, suppose that we pick a subset Z of the co-ordinates, with the property that when two elementary normal discs are incompatible, at least one of their co-ordinates lies in Z. Consider the set of vectors with real nonnegative entries that satisfy the matching equations and that satisfy the extra condition that whenever a co-ordinate lies in Z, it is forced to be zero. We denote this set by $\mathcal{N}_Z$. Then $\mathcal{N}_Z$ is simply the intersection of a subspace of $\mathbb{R}^k$ with the nonnegative quadrant $\{(x_1, \ldots, x_k) : x_i \geq 0 \ \forall i\}$. Hence, it is a cone on a compact polytope. This polytope is just the intersection of this set with the hyperplane $\{(x_1, \ldots, x_k) : x_1 + \cdots + x_k = 1\}$. We denote it by P_Z. Note that $\mathcal{N}$ is the union of $\mathcal{N}_Z$ over all possible subsets Z.

Let S, S_1 and S_2 be properly embedded normal surfaces. Then S is said to be the *sum* of S_1 and S_2 if $[S] = [S_1] + [S_2]$. We often write $S = S_1 + S_2$. The sum of n parallel copies of S is denoted by nS. Now, the Euler characteristic of S is a linear function of the number of elementary normal discs of each type. Hence, when $S = S_1 + S_2$, then $\chi(S) = \chi(S_1) + \chi(S_2)$.

The normal surface S is a *vertex surface* if it is connected, and whenever nS is the sum of S_1 and S_2 for some positive integer n, then each of S_1 and S_2 is a multiple of S.

5.3. *Realising certain surfaces as vertex surfaces.* Jaco and Tollefson [20] proved that many topologically relevant surfaces may in fact be realised as vertex surfaces. One of their results is as follows (see [20, Lemma 5.1]).

THEOREM 5.4. *Let M be a compact orientable 3-manifold with a triangulation T. Suppose that M is reducible. Then there is a vertex normal surface S that is a reducing sphere, such that $w(S)$ is minimal among all reducing spheres that are in general position with respect to the 1-skeleton.*

We will need a variation on this result, which differs from it in two ways. Firstly, we will not be dealing with a triangulation. Instead, we will start with a triangulation $\mathcal{T}$ (of the 3-sphere) in which the link L is simplicial, and we will remove a small regular neighbourhood of L, forming a polyhedral structure $\mathcal{P}$. Now, many of Jaco and Tollefson's arguments do not extend from triangulations to polyhedral structures. However, any *closed* normal surface in $\mathcal{P}$ is also normal in $\mathcal{T}$. The arguments of Jaco and Tollefson do work in this

setting. Secondly, we will use a slightly more refined version of complexity, as in Theorem 5.1. We therefore obtain the following result. The proof of this precisely follows that of Lemmas 5.1 and 4.8 in [20] and is omitted.

THEOREM 5.5. *Let $\mathcal{T}$ be a triangulation of a compact orientable 3-manifold. Let M be the compact 3-manifold that results from removing a small open neighbourhood of a subcomplex L of the 1-skeleton. Let $\mathcal{P}$ be the resulting polyhedral structure. Let β be a subcomplex of the 1-skeleton of $\mathcal{P}$. Suppose that M is reducible. Then there is a reducing sphere that is a vertex normal surface with respect to $\mathcal{T}$, and such $(w_\beta(S), w(S))$ is minimal among all reducing spheres that are in general position with respect to the 1-skeleton.*

5.4. *Boundary-vertex surfaces.* When dealing with vertex surfaces, one loses some control over their boundary behaviour. In order to get around this, we introduce a new notion.

Let M be a compact orientable 3-manifold with a polyhedral decomposition $\mathcal{P}$. Let S be a properly embedded normal surface in M. Then S is a *boundary-vertex surface* if S is connected, and whenever nS is the sum of normal surfaces S_1 and S_2, where ∂S_1 and ∂S_2 are both multiples of ∂S, then each of S_1 and S_2 is a multiple of S.

Boundary-vertex surfaces will play an important role in the proof of our theorems in the case of the unknot. We will therefore explore them in some detail now.

Fix a collection of disjoint simple closed curves C in ∂M that are normal. The *C-normal surface solution space* $\mathcal{N}^C$ is the set of vectors in the normal solution space $\mathcal{N}$ with boundary that is a multiple of C.

As in the case of the usual normal surface solution space, $\mathcal{N}^C$ is a union of convex polytopes glued along certain faces. This is because a vector in $\mathcal{N}$ lies in $\mathcal{N}^C$ if and only if it satisfies a collection of extra linear equations. Consider two different arc types of normal arcs in the 2-cells of ∂M. Let c_i and c_j be the number of arcs of C of these two types. For a normal surface S, the number of arcs in ∂S of these two types are linear functions ϕ_i and ϕ_j of $[S]$. So, to lie in $\mathcal{N}^C$, $[S]$ must satisfy the linear equation $c_j\phi_i[S] = c_i\phi_j[S]$. These equations, as we run over all pairs of arc types in ∂M, give the extra conditions required to determine $\mathcal{N}^C$. Now, just as $\mathcal{N}$ is a union of the polytopes $\mathcal{N}_Z$, we may form similar polytopes $\mathcal{N}_Z^C$ with the above extra linear constraints. So, $\mathcal{N}_Z^C = \mathcal{N}^C \cap \mathcal{N}_Z$. Then $\mathcal{N}^C$ is the union of $\mathcal{N}_Z^C$ over all possible Z. Note that $\mathcal{N}_Z^C$ is a cone over a compact polytope, where the compact polytope is again the intersection with $\{(x_1, \dots, x_k) : x_1 + \cdots + x_k = 1\}$. We denote this compact polytope by P_Z^C.

The condition that S is a boundary-vertex surface is precisely that $[S]$ is a multiple of a vertex of some $P_Z^{\partial S}$ and that S is connected. The reason for

this is as follows. Suppose that $[S]$ is a multiple of a vertex of some $P_Z^{\partial S}$ and that $nS = S_1 + S_2$ where ∂S_1 and ∂S_2 are both multiples of ∂S. Then, for each co-ordinate of S that is zero, the corresponding co-ordinates of S_1 and S_2 are zero. So, S_1 and S_2 both lie in $\mathcal{N}_Z^{\partial S}$, and so some multiples of these surfaces lie in $P_Z^{\partial S}$. However, since S is a multiple of a vertex of $P_Z^{\partial S}$, we deduce that both S_1 and S_2 are multiples of S. Conversely, suppose that $[S]$ is not a multiple of any vertex of any $P_Z^{\partial S}$. Let Z be the set of zero co-ordinates of S. Then a multiple $k[S]$ lies in $P_Z^{\partial S}$ for some positive real k. It can therefore be expressed as an affine linear combination $\lambda_1 v_1 + \cdots + \lambda_n v_n$ of the vertices of $P_Z^{\partial S}$, where $\lambda_1 + \cdots + \lambda_n = 1$ and each λ_i is nonnegative. Choose such an expression where as many of the λ_i as possible are zero. After re-ordering, we express $k[S]$ as $\lambda_1 v_1 + \cdots + \lambda_m v_m$ where each λ_i is positive. Since m is minimal, the coefficients $\lambda_1, \ldots, \lambda_m$ are uniquely determined. Hence, they are the unique solution to a system of linear equations with rational coefficients, and therefore they are rational. Rescaling, we obtain S as a nontrivial sum of surfaces, each with boundary a multiple of ∂S, none of which is a multiple of S. Thus, S is not a boundary-vertex surface.

We will need to realise compression discs as boundary-vertex surfaces. The precise result, which is an analogue of Theorem 5.5, is as follows.

THEOREM 5.6. *Let M be a compact orientable irreducible 3-manifold with a polyhedral decomposition $\mathcal{P}$ and a subcomplex β in its 1-skeleton. Suppose that ∂M is compressible, and let C be an essential normal simple closed curve in ∂M that bounds a disc in M. Suppose that, for each edge in ∂M, all points of intersection between C and that edge have the same sign. Then there exists a normal disc S bounded by C such that*

(1) *S is a boundary-vertex surface; and*
(2) *$(w_\beta(S), w(S))$ is minimal among all normal discs with boundary equal to C.*

We will now embark upon a proof of this. As mentioned above, the arguments of Jaco and Tollefson in [20] do not readily translate to the polyhedral setting. We therefore provide a more direct argument.

We need the following lemma. This is proved in exactly the same way as Lemma 2.1 in Jaco and Oertel [19], to which we refer the reader for a proof.

LEMMA 5.7. *Let M be a compact orientable irreducible 3-manifold with a polyhedral decomposition $\mathcal{P}$ with a subcomplex β in its 1-skeleton. Let S be a properly embedded, incompressible, normal surface such that $(w_\beta(S), w(S))$ is minimal among all surfaces isotopic to S via an isotopy that keeps ∂S fixed. Suppose that $S = S_1 + S_2$ and that the number of components of $S_1 \cap S_2$ is minimal among all normal surfaces S_1' and S_2' such that $\partial S_1' = \partial S_1$, $\partial S_2' = \partial S_2$, S_1' and S_2' are isotopic to S_1 and S_2 keeping their boundaries fixed and*

$S = S_1' + S_2'$. Then no component of $S_1 \cap S_2$ is a simple closed curve bounding a disc in S_1 or S_2.

COROLLARY 5.8. *Let M be a compact orientable irreducible 3-manifold M with a polyhedral decomposition $\mathcal{P}$ with a subcomplex β in its 1-skeleton. Let S be a properly embedded, incompressible, normal surface such that $(w_\beta(S), w(S))$ is minimal among all surfaces isotopic to S via an isotopy that keeps ∂S fixed. Then S cannot be written as $S_1 + S_2$, where S_2 is a 2-sphere.*

Proof. We may assume that $S_1 \cap S_2$ is minimal among all normal surfaces S_1' and S_2' such that $\partial S_1' = \partial S_1$, $\partial S_2' = \partial S_2$, S_1' and S_2' are isotopic to S_1 and S_2 keeping their boundaries fixed and $S = S_1' + S_2'$. Since S_2 is a 2-sphere, each component of $S_1 \cap S_2$ bounds a disc in S_2, which contradicts Lemma 5.7. □

Proof of Theorem 5.6. By Theorem 5.2, there is a compression disc S in normal form, with $\partial S = C$, such that $(w_\beta(S), w(S))$ is minimal among all compression discs that are in general position with respect to the 1-skeleton and that have boundary equal to C.

Note that this implies that, for each positive integer n, $(w_\beta(nS), w(nS))$ is minimal among all collections of n disjoint discs with boundary equal to nC. For if there was a collection of n such discs with smaller complexity, then one of these discs would have to have complexity less than that of S, which is a contradiction.

Now, $[S]$ lies in the C-normal solution solution space. It therefore lies in some polytope $\mathcal{N}_Z^C$. This is a cone on the compact polytope P_Z^C. Let λ be the unique real number such that $\lambda[S] \in P_Z^C$. Now, P_Z^C is the affine hull of its vertices $v_1, \dots, v_m$. Hence, there are nonnegative real numbers $\lambda_1, \dots, \lambda_m$ that sum to 1 such that $\lambda_1 v_1 + \dots + \lambda_m v_m = \lambda[S]$. Suppose that as many of the λ_i as possible are zero. We may assume that the first k of them, say, are nonzero and the remainder are zero. So, $\lambda_1 v_1 + \dots + \lambda_k v_k = \lambda[S]$. Divide by λ to get an expression $\mu_1 v_1 + \dots + \mu_k v_k = [S]$. By our minimality assumption, these real numbers $\mu_1, \dots, \mu_k$ are unique. Now each v_i has rational co-ordinates and so because of the uniqueness of the μ_is, each μ_i is therefore rational. Hence, clearing denominators, we get an expression

$$n_1[S_1] + \dots + n_k[S_k] = nS.$$

Here, each S_i is a connected C-normal surface, which is a boundary-vertex surface. Also, n and each n_i is a positive integer. Hence,

$$n_1\chi(S_1) + \dots + n_k\chi(S_k) = n\chi(S).$$

Since each S_i is C-normal, its boundary consists of multiples of C. So,

$$n_1|\partial S_1| + \dots + n_k|\partial S_k| = n|\partial S| = n.$$

Therefore,

$$n_1(\chi(S_1) - |\partial S_1|) + \dots + n_k(\chi(S_k) - |\partial S_k|) = 0.$$

There are therefore two cases:

(1) for some i, $\chi(S_i) > |\partial S_i|$;
(2) for each i, $\chi(S_i) = |\partial S_i|$.

Let us consider Case (1) first. Let $\hat{S}_i$ be the result of attaching a disc to each boundary component of S_i. Then $\chi(\hat{S}_i) = \chi(S_i) + |\partial S_i| > 2|\partial S_i|$. But $\hat{S}_i$ is a closed connected surface, and so its Euler characteristic is at most 2. We deduce that $|\partial S_i| = 0$. Thus, S_i is a 2-sphere or projective plane. Now, S_i cannot be a projective plane, for a regular neighbourhood would be a punctured $\mathbb{R}P^3$, which would force M to be reducible, and this is contrary to assumption. Therefore, S_i is a 2-sphere. We hence get an expression $nS = S_i + W$ for some normal surface W. By Corollary 5.8, this is impossible.

Let us now consider Case (2). Then each S_i is a disc, torus or Klein bottle. We claim that, in fact, no S_i is a torus or Klein bottle. Suppose it were. Write $nS = S' + S_i$. Then S' has the same boundary and the same Euler characteristic as nS. It cannot have any 2-sphere or projective plane components, for this would contradict Corollary 5.8 or irreducibility. Hence, it consists of n discs, plus possibly some tori and Klein bottles. Let S'' be the union of the disc components of S'. Then the total complexity of S'' is strictly less than that of nS. Therefore, some component of S'' has strictly smaller complexity than S. This is a contradiction.

We deduce that each S_i must be a disc. So,

$$n_1 + \cdots + n_k = n_1\chi(S_1) + \cdots + n_k\chi(S_k) = n\chi(S) = n.$$

Now,

$$n_1 w_\beta(S_1) + \cdots + n_k w_\beta(S_k) = n w_\beta(S).$$

Since each S_i is a disc with boundary equal to C, the minimality assumption on $(w_\beta(S), w(S))$ implies that $w_\beta(S_i) \geq w_\beta(S)$. Hence,

$$n w_\beta(S) = (n_1 + \cdots + n_k) w_\beta(S) \geq n_1 w_\beta(S_1) + \cdots + n_k w_\beta(S_k) = n w_\beta(S).$$

We deduce that, for each i, $w_\beta(S_i) = w_\beta(S)$. Applying the same argument, we also deduce that $w(S_i) = w(S)$. Hence, each S_i is a normal disc with boundary C and with minimal complexity. Any of these is our required boundary-vertex surface. □

5.5. *Estimating the size of normal surfaces.* The following is due to Hass, Lagarias and Pippenger (Lemma 6.1 in [14]).

THEOREM 5.9. *Let M be a compact 3-manifold with a triangulation having t tetrahedra. Then, each vertex normal surface S, where $[S] = (x_1, \ldots, x_{7t})$, satisfies*

$$\max_{1 \leq i \leq 7t} |x_i| \leq 2^{7t-1}.$$

We will need the following version of this for compressing discs in polyhedral decompositions.

THEOREM 5.10. *Let M be a compact orientable 3-manifold with a polyhedral decomposition. Let c be an upper bound for the number of elementary normal disc types in each polyhedron, and let k be the number of elementary disc types in total. Let S be a compression disc for ∂M that is a normal boundary-vertex surface. Let $(x_1, \dots, x_k)$ be the vector $[S]$. Let $y_1, \dots, y_\ell$ denote the weights of the edges in ∂M. Then*

$$\max_{1 \leq i \leq k} |x_i| \leq (2c)^{k-1} \left(\sum_{i=1}^{\ell} |y_i| \right).$$

Proof. Consider the following set of linear equations:

(1) the matching equations,
(2) the equation $x_i = 0$ for each co-ordinate where $[S]_i$ is zero,
(3) the equations that specify that $x_i = [S]_i$ for all edges in ∂M.

These can be expressed as $Ax = y$, where A is a matrix, $x = (x_1, \dots, x_k)^T$ and y is a column vector with the first set of entries being zero and the remaining entries being the co-ordinates $y_1, \dots, y_\ell$ of $[\partial S]$. Now, since S is a boundary-vertex surface, the only solution to these equations is $[S]$. Hence, A has zero kernel. So, its rank equals the number of columns. Hence, we may find a square submatrix B with the same number of columns and with nonzero determinant. The equations corresponding to the rows of B become $Bx = y'$ for a submatrix y' of y. Inverting, we get $x = B^{-1}y'$. Now, the rows of B have entries that are 0, 1 and -1, and there are at most $2c$ nonzero entries in each row. Also, B^{-1} equals $\mathrm{adj}(B)/\det(B)$, where $\mathrm{adj}(B)$ is the adjugate matrix. Since B has integral entries and nonzero determinant, $|\det(B)| \geq 1$. Each entry of $\mathrm{adj}(B)$ is a determinant of a minor of B and so has modulus at most $(2c)^{k-1}$. The required bound on the modulus of each co-ordinate of x immediately follows. □

5.6. *Normally parallel surfaces.* Another useful feature of normal surfaces is that it is possible to speak of parts of the surface as being normally parallel. The formal definition of this is as follows.

Let M be a compact 3-manifold with a polyhedral decomposition $\mathcal{P}$. Let S be a (possibly disconnected) surface properly embedded in M that is in normal form with respect to $\mathcal{P}$. Then two subsurfaces S_0 and S_1 of S are said to be *normally parallel* if there are subsurfaces S_0' and S_1' of S, each of which is a union of elementary normal discs, and satisfying $S_0' \supseteq S_0$ and $S_1' \supseteq S_1$, and an embedding $H \colon S_0' \times [0,1] \to M$ such that the following hold:

(1) for each elementary normal disc D of S_0' and each $t \in [0,1]$, $H(D,t)$ is an elementary normal disc;
(2) $H(S_0' \times \{i\}) = S_i'$ for $i = 0$ and 1,
(3) $H(S_0 \times \{i\}) = S_i$ for $i = 0$ and 1.

6. **Triangulations and arc presentations**

6.1. *Dynnikov's triangulation.* Dynnikov gave a triangulation of the 3-sphere associated with an arc presentation of a link L. In this subsection, we describe this triangulation.

As in Section 2, the 3-sphere is viewed as a join $S^1_\theta * S^1_\phi$. Let n be the arc index of the arc presentation. Then L intersects the binding circle S^1_ϕ in n points. The intersection between each page $\mathcal{D}_t$ and L is either empty or a single open arc. In the latter case, we may assume that this arc is a concatenation of two arcs that are joined at S^1_θ. We may take each of these arcs to be (ϕ, τ, θ) for fixed θ and ϕ and with τ varying between 0 and 1.

With L in this form, we now define the triangulation of S^3 in which L is simplicial. If $s_1 < \cdots < s_n$ are the vertices $L \cap S^1_\phi$ and $t_1 < \cdots < t_n$ are the points $L \cap S^1_\theta$, we subdivide S^1_ϕ and S^1_θ at these points. We choose the parametrisation of θ and ϕ so that these points are equally spaced around S^1_ϕ and S^1_θ. Thus, each circle has been subdivided into n 1-simplices. We give S^3 the triangulation that is the join of these two triangulations of S^1_ϕ and S^1_θ. A typical 3-simplex is therefore of the form $[s_i, s_{i+1}] * [t_j, t_{j+1}]$, for 1-simplices $[s_i, s_{i+1}] \subset S^1_\phi$ and $[t_j, t_{j+1}] \subset S^1_\theta$, where the indexing is mod n.

This triangulation $\mathcal{T}$ will be of crucial importance in this paper. In the case where L is a split link, we will arrange that a splitting 2-sphere is normal with respect to $\mathcal{T}$. However, when L is the unknot, the characteristic surface is a spanning disc that cannot be made normal with respect to $\mathcal{T}$ since L is a subset of the 1-skeleton. It is therefore necessary to work with a modified version of the triangulation, which we define in the next subsection.

6.2. *A modification of the triangulation.* The first thing that we do is replace each 1-simplex in S^1_θ and S^1_ϕ by two 1-simplices. We again work with the triangulation of the 3-sphere that is the join of these triangulations. We denote this also by $\mathcal{T}$. This has $4n^2$ tetrahedra. The purpose of doing this is so that, for each tetrahedron Δ, $L \cap \Delta \cap S^1_\phi$ is at most one point, and similarly $L \cap \Delta \cap S^1_\theta$ is at most one point. Hence, for each tetrahedron Δ, the intersection $\Delta \cap L$ is now at most two isolated points or a single edge.

We now remove a regular neighbourhood of L. The effect of this on each tetrahedron is to truncate some vertices or slice off an edge. This is shown in Figure 21. This converts each tetrahedron into a polyhedron. Let $\mathcal{P}$ denote the resulting polyhedral decomposition of the exterior of L.

6.3. *The number of elementary disc types.* In this subsection, we provide the following crude upper bound on the number of elementary normal disc types in each polyhedron of $\mathcal{P}$.

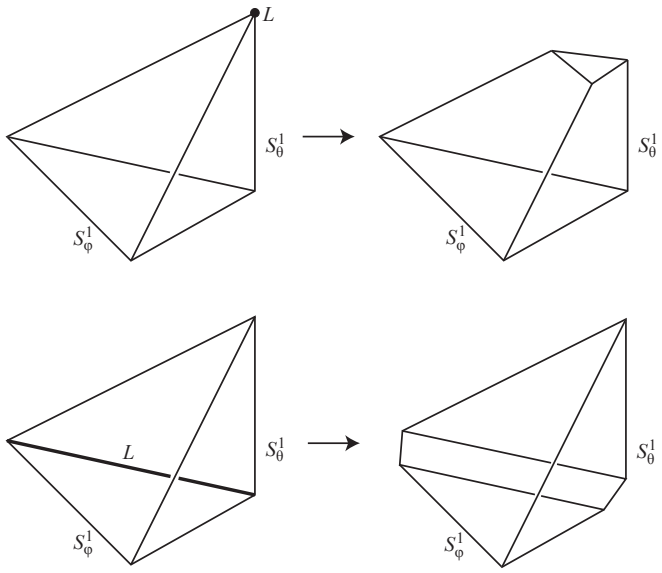

Figure 21. Truncating the tetrahedra

LEMMA 6.1. *The number of elementary normal disc types in each polyhedron of* $\mathcal{P}$ *is at most* 10^6.

Proof. Each face of $\mathcal{T}$ is a triangle. When truncated to form $\mathcal{P}$, this face ends up with at most five sides. Since an elementary normal disc can intersect each edge at most once, it therefore intersects this face in at most two normal arcs. There are at most ten ways of inserting two normal arcs into the face (since these avoid at most one of the edges, and this avoided edge determines the normal arcs up to one further choice). There are at most ten ways of inserting one normal arc. Hence, there are at most 21 possible configurations for the intersection between the face and an elementary normal disc. The normal disc is almost determined by its intersection with these four faces. The one ambiguity is when L intersects the tetrahedron in an edge, which is sliced off to form a rectangular face. Then when the elementary normal disc intersects all four edges of this rectangular face, there are two possible ways that it can intersect this face. So, there are at most $2 \times 21^4 < 10^6$ possible elementary normal disc types in each polyhedron. □

6.4. *The specified longitude.* The boundary $\partial N(L)$ of this polyhedral structure inherits a cell structure. Each truncated vertex of a tetrahedron gives rise to a triangular 2-cell. Each sliced-off edge gives rise to a rectangular 2-cell.

In the case where L has a single component, we will now pick a normal, simple closed curve C in $\partial N(L)$ that has winding number one along $N(L)$ and zero linking number with L. We will term this curve the *specified longitude*.

We first create a normal curve C' in $\partial N(L)$ that has winding number one along $N(L)$, but not necessarily zero linking number with L.

Now L is a union of arcs, each of which is the closure of the intersection with some page. When the arc index n is even, we label these arcs alternately as *up* and *down* arcs. When the arc index n is odd, this is not possible, and so we label the arcs as alternately *up* and *down*, with the exception of one arc that is unlabelled. We also pick an orientation on L.

It is also the case that L is a union of edges of the triangulation $\mathcal{T}$. For each edge, there are four rectangular 2-cells in $\partial N(L)$ that encircle it. Two of these rectangles have slightly greater θ-values than the arc of L; two have slightly smaller θ-values. Similar statements are true for the ϕ-values. We now label the edges of L in this triangulation. If the edge lies in a labelled arc, we give it the same label. If the edge lies in an unlabelled arc, then we consider the labelled arc to which it is incident and give it the opposite label. Now arrange C' in the neighbouring rectangles according to the following recipe:

(1) if the edge of L is labelled 'up' and runs from S^1_ϕ to S^1_θ, then choose C' in this neighbourhood to have slightly greater θ-value and slightly greater ϕ-value;
(2) if the edge of L is labelled 'up' and runs from S^1_θ to S^1_ϕ, then choose C' in this neighbourhood to have slightly greater θ-value and slightly smaller ϕ-value;
(3) if the edge of L is labelled 'down' and runs from S^1_ϕ to S^1_θ, then choose C' in this neighbourhood to have slightly smaller θ-value and slightly smaller ϕ-value;
(4) if the edge of L is labelled 'down' and runs from S^1_θ to S^1_ϕ, then choose C' in this neighbourhood to have slightly smaller θ-value and slightly greater ϕ-value.

At each point of $L \cap S^1_\theta$ or $L \cap S^1_\phi$, there is a collection of triangles of $\partial N(L)$. Coming into these, there are the endpoints of two arcs of C' lying in rectangular 2-cells. Join these by a path of normal arcs in the triangles that is as short as possible. (At the point of $L \cap S^1_\theta$ in the middle of the unlabelled arc, C' will also need to cross some rectangular 2-cells.) The result is the simple closed curve C'.

Suppose that the rectangular diagram associated with this arc presentation has writhe k. Then we claim that the modulus of the linking number between C' and L is at most $|k| + n + 1$. We see that C' runs parallel to each vertical and horizontal edge of the rectangular diagram, except possibly at the midpoint of just one edge, where it may jump from one side of the edge to the other. This exceptional case will correspond to the arc of L containing a boundary saddle. When vertical and horizontal arcs of the diagram meet at their endpoints, a crossing between C' and L can occur. We deduce that

$\mathrm{lk}(C', L)$ differs from the writhe of the rectangular diagram by at most $n+1$. Therefore, $|\mathrm{lk}(C', L)| \leq |k| + n + 1$, as claimed. Note that $|k|$ is at most the number of crossings of the rectangular diagram, which is at most $(n-1)^2$, and so we also deduce that $|\mathrm{lk}(C', L)| < n^2$.

To obtain C, we perform some Dehn twists to C', the twisting curve being a meridian that encircles L half-way along an edge of L. If L has an unlabelled arc, then choose the twisting curve to be a meridian of one of its edges. We perform enough Dehn twists so that $\mathrm{lk}(C, L) = 0$.

We say that the number of Dehn twists that we performed is the *twisting number* of C. Hence, this number is at most $|k| + n + 1$.

It is a consequence of the construction that C is normal in $\partial N(L)$ and that, for each edge of the cell structure of $\partial N(L)$, C intersects that edge in points of the same sign.

We now estimate the weight of C, which is the number of points of intersection with the 1-skeleton of $\mathcal{P}$. The number of triangles of $\partial N(L)$ at each 0-cell of L is $4n - 8$. By construction, C' runs through at most $2n$ of these. Therefore, the weight of C' is at most $4n^2$. The creation of C from C' introduces at most $4n^2$ points of intersection. So, the weight of C is at most $8n^2$.

6.5. *Making the elementary normal discs piecewise-linear.* Each 3-simplex of $\mathcal{T}$ may be identified with a Euclidean tetrahedron, since it is the join of two edges (one lying in S^1_θ, the other lying in S^1_ϕ), which we may take to be Euclidean straight lines. Each polyhedron in $\mathcal{P}$ is a subset of a tetrahedron in $\mathcal{T}$, which we may choose to be convex. We may also choose the gluing maps between the faces of adjacent polyhedra to be isometries.

Our goal in this subsection is to realise each elementary normal disc of a normal surface as piecewise-linear, with respect to the Euclidean structure on the polyhedron that contains it. So, consider a surface S properly embedded in the exterior of L that is normal with respect to $\mathcal{P}$.

We first arrange the points of $S \cap S^1_\theta$ in a certain way. We have arranged that each 1-simplex in S^1_θ and S^1_ϕ has equal length. We first ensure that each point of $S^1_\theta \cap S$ lies in the middle half of the 1-simplex in S^1_θ that contains it. In other words, it lies closer to the midpoint of this 1-simplex than to either of its endpoints. This will be technically convenient later in the argument.

We next arrange for S to intersect each face of $\mathcal{P}$ in straight arcs, without moving their endpoints. We then arrange for S to lie inside each polyhedron P of $\mathcal{P}$ in a certain way. The boundary of the elementary normal discs is a union of normal arcs in ∂P, which we have taken to be straight in the Euclidean structure. The elementary normal discs that are triangles can then be realised as flat. The elementary normal squares can each be realised as two flat triangles, joined along a straight line. We call these two triangles *half-squares*. When the square intersects S^1_θ and S^1_ϕ, we choose this straight line

so that it runs between S^1_θ and S^1_ϕ. We can choose the straight lines in the remaining squares so that the union of the squares is embedded.

When a normal surface S is closed, its piecewise-linear structure is now completely determined. However, when S has nonempty boundary, there are many more types of elementary disc to consider. We realise these as piecewise-linear in the following way.

Cut the polyhedron P along a thin regular neighbourhood of the triangles and squares in $S \cap P$, creating a union of (possibly nonconvex) polyhedra. Each such polyhedron P' is star-shaped, centred at some point v, say, in its interior. Create a collection of copies of $\partial P'$ by performing dilations based at v with dilation factor smaller than 1. We create as many copies as there are components of $S \cap \mathrm{int}(P')$. The curves $S \cap \partial P'$ are simple closed curves in the sphere $\partial P'$. Hence, there is one, α, that is innermost in $\partial P'$. Attach to α an annulus that runs to the outermost dilated copy of $\partial P'$. Take this annulus to be a subset of a cone on α with cone point v. Now attach, to the other boundary component of the annulus, the disc in the dilated copy of $\partial P'$ that it bounds. The resulting disc is the required piecewise-linear elementary normal disc spanned by α. Repeat this procedure with a curve in $(S \cap \partial P') - \alpha$ that is innermost in $\partial P'$, but this time using the second-outermost dilated copy of P'. Continuing in this fashion, we realise all of $S \cap P'$ as piecewise-linear.

6.6. PL-*admissible form.* Let S be a surface properly embedded in the exterior of L that is normal with respect to $\mathcal{P}$ and that is piecewise-linear. As in the case of admissible form, this surface S inherits a singular foliation $\mathcal{F}$ on $S - S^1_\phi$ defined by $d\theta = 0$. (See Figure 22 for example.)

The normal surface is not admissible for many reasons. It is piecewise-linear, not smooth. We have yet to make sense of a 'singularity' for such a piecewise-linear surface, but with any reasonable definition, its singularities

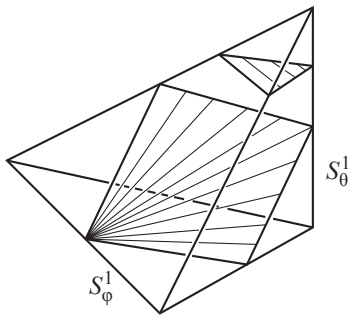

Figure 22. Some elementary normal discs with their foliation

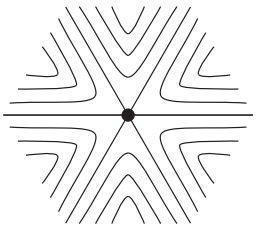

Figure 23. A generalised saddle

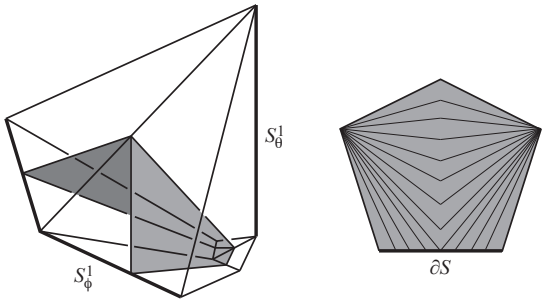

Figure 24. Foliation near the boundary

cannot be said to be of 'Morse type.' Finally, it need not have the correct behaviour near ∂S. In this subsection, we introduce the notion of PL-admissible form; the normal surface will have this structure.

Consider a piecewise-linear surface S embedded in $\mathbb{R}^3$ with height function h given by the final co-ordinate. Suppose that no 1-cell of S is horizontal with respect to h. A point p in S is *nonsingular* (with respect to h) if it has a disc neighbourhood N in S such that $\{x \in N : h(x) = h(p)\}$ is a properly embedded arc in N, running through p. Otherwise p is *singular*. We say that a singular point p is a *pole* if it has a neighbourhood N such that $\{x \in N : h(x) = h(p)\}$ is just $\{p\}$.

Note that the singular points are isolated. The ones that are not poles are *generalised saddles*. An example of the singular foliation near a generalised saddle is shown in Figure 23. A generalised saddle p has a disc neighbourhood N such that $\{x \in N : h(x) = h(p)\}$ is a star-shaped graph with central vertex p. When $p \in S - \partial S$, the number of edges of this graph coming out of p is an even integer at least 4. When this integer is 4, we say that p is a *saddle*. When $p \in \partial S$, the number of edges coming out of p is an integer at least 2. When this is 2, we say that p is a *boundary-saddle* (see Figure 24).

A surface S properly embedded in the exterior of L is *PL-admissible* if the following hold:

(1) it is piecewise-linear in each polyhedron of $\mathcal{P}$;
(2) it intersects the binding circle transversely at finitely many points;

(3) with respect to the function θ on $S^3 - S^1_\phi$, S has no horizontal 1-cells and finitely many singularities;
(4) each page contains at most one arc of L and at most one singularity of S, but not both.

We can translate the terminology of admissible surfaces to this setting. A *vertex* of S is a point of $S \cap S^1_\phi$. When the singularities are removed from the singular foliation $\mathcal{F}$ on $S - S^1_\phi$, the result is a genuine foliation. Each leaf is a *fibre*. A fibre that is incident to a generalised saddle is a *separatrix*. Each component of the complement of the vertices, the singular locus and the separatrices is a *tile*. For a vertex s of $\mathcal{F}$, the closure of the union of all the fibres approaching s is the *star* of s. The *valence* of s is the number of separatrices approaching s.

Note that PL-admissible surfaces have quite different behaviour near the boundary than in the case of admissible surfaces. This is for several reasons. In the case of admissible surfaces, their boundary is L, which is a union of arcs in pages. On the other hand, PL-admissible surfaces lie in the exterior of L and hence have boundary on $\partial N(L)$. Their boundary curves need not be union of horizontal arcs. In fact, they have no horizontal arcs in their boundary because of the assumption that no 1-cell is horizontal. An example of the singular foliation near ∂S is shown in Figure 24.

Let S be a normal surface that has been made piecewise-linear as described in Section 6.5.

LEMMA 6.2. *In the interior of each elementary normal disc of S, there are at most* 24 *singularities. Of these, at most* 12 *are generalised saddles, and all of these are saddles.*

Proof. Note first that a singularity in the interior of a piecewise-linear surface only occurs when more than two flat discs meet at a point. Moreover, at least four such discs have to meet a point for this to be a generalised saddle. At least six such discs have to meet for the point to be a generalised saddle that is not a saddle.

Let D be an elementary normal disc. When D is a triangle or square, it has no singularities in its interior. So suppose that D is not of this form. Then in our construction, D consists of two parts: an annulus A that runs between ∂D and a dilated copy of ∂D, and a disc that is a subset of a dilated polyhedron. Singularities that lie in $A - \partial D$ must lie in $\partial A - \partial D$, and these have at most four flat discs incident to them. So, any such singular points must be poles or saddles. The number of such singularities is at most the number of points of intersection between ∂D and the 1-skeleton of $\mathcal{P}$, which is at most 12, since this is the maximal number of edges of a polyhedron in $\mathcal{P}$. The vertices in the interior of the disc part of D correspond to vertices of the polyhedron.

It is easy to check that there are at most 12 of these. None of these can be a generalised saddle because they all have three flat discs incident to them. □

LEMMA 6.3. *Each singular point in ∂S has at most two fibres incident to it, and so is a boundary-saddle or a pole.*

Proof. Each elementary normal disc is flat near ∂S. So the only way that a singularity can appear on ∂S is at the intersection between two elementary normal discs. Since just two flat discs meet here, this implies that the singular point has precisely two or zero fibres incident to it. (See Figure 24.) □

6.7. *Exceptional and typical separatrices.* An example of a separatrix is shown in Figure 22, running in the elementary normal square from S^1_θ to S^1_ϕ. We say that a separatrix that lies entirely in an elementary normal square is *typical*. Otherwise, it is *exceptional*.

LEMMA 6.4. *There are at most $408n^2$ exceptional separatrices of S.*

Proof. Each exceptional separatrix emanates from a generalised saddle. There are three possible locations for a generalised saddle: on the boundary of S, in the interior of an elementary normal disc and on S^1_θ. We consider these generalised saddles in turn.

The weight of C is at most $8n^2$. Hence, the number of singularities on ∂S is at most $8n^2$. By Lemma 6.3, each gives rise to at most two exceptional separatrices.

When a generalised saddle lies in the interior of an elementary normal disc, this normal disc cannot be a triangle or square, and so it must intersect $\partial N(L)$. There are at most $8n^2$ such discs. Each contains at most 12 generalised saddles in its interior, all of which are saddles, by Lemma 6.2. So, these give rise to at most $384n^2$ exceptional separatrices.

The remaining separatrices are incident to S^1_θ. To be an exceptional separatrix, it must start in an elementary normal disc that is not a triangle or square. There are at most $8n^2$ of these, and each such disc intersects S^1_θ at most once. So, we obtain at most $8n^2$ exceptional separatrices of this form. This gives a total at most $408n^2$ exceptional separatrices. □

6.8. *Ordinary tiles and deep vertices.* We say that a tile of S is *ordinary* if it satisfies the following conditions:

(1) its closure is a disc disjoint from ∂S,
(2) its boundary is a union of typical separatrices,
(3) it lies in the union of the elementary squares and triangles.

LEMMA 6.5. *The number of disc tiles that are not ordinary is at most $1644n^2$. Moreover, if S is closed, then every disc tile is ordinary.*

In order to prove this, we will need to introduce the following definition. For a disc tile T of S, we define its *θ-width* as follows. Let s_1 and s_2 be its vertices. Pick a properly embedded arc γ in T with endpoints in distinct components of $\partial T - \{s_1, s_2\}$. Then the θ-width of the tile is $\left|\int_\gamma d\theta\right|$.

LEMMA 6.6. *For all disc tiles with at most* $816n^2$ *exceptions, the tile has* θ*-width at least* $\pi/2n$.

Proof. By Lemma 6.4, there are at most $408n^2$ exceptional separatrices, and these lie in the boundary of at most $816n^2$ tiles. Therefore, consider a tile that has no exceptional separatrix in its boundary. Consider a vertex s of the tile. The two singular fibres in the boundary of the tile emanating from s lie in elementary normal squares. These lie in distinct tetrahedra of $\mathcal{T}$. There are at most $2n$ tetrahedra arranged around the 1-simplex containing s. They each account for θ-angle around that 1-simplex of at least $2\pi/2n$. Since we have arranged that each point of intersection between S and S^1_θ lies in the middle half of the 1-simplex that contains it, we deduce that the difference in θ value between these two singular fibres is at least $2\pi/4n$. □

Proof of Lemma 6.5. If a disc tile is not ordinary, either its closure intersects ∂S or it contains an exceptional separatrix in its boundary.

We say that a tile is a *boundary-tile* if it intersects ∂S in an arc. Not all tiles with closure that intersects ∂S need be boundary-tiles. This is because the closure of a tile can intersect ∂S at isolated points, which are boundary saddles. But there are at most $8n^2$ of these.

We claim that there are at most $820n^2$ boundary-tiles. The total θ-width of the boundary tiles equals the total θ-angle that C runs through; in other words, $\int_C |d\theta|$. Now, C is a union of normal arcs in $\partial N(L)$. As C runs along rectangular faces of $\partial N(L)$, its θ-angle barely changes, except near the endpoints of the rectangle that lie near S^1_ϕ. At these endpoints, it then runs through triangular faces of $\partial N(L)$. As it does so, its change in θ-angle is at most 2π. So, the total θ-angle that C runs through is at most 2π times the number of vertices of L; in other words, $2\pi n$. Now, for all but at most $816n^2$ tiles, the θ-width of the tile is at least $\pi/2n$, by Lemma 6.6. So, the number of boundary-tiles is at most $816n^2 + 4n^2 = 820n^2$, as claimed.

Finally, each exceptional separatrix lies in the boundary of two tiles. So, by Lemma 6.4, this gives rise to at most $816n^2$ tiles that are not ordinary. □

We say that two vertices of $S \cap S^1_\phi$ are of the same *type* if their stars are normally parallel. We say that a vertex is *deep* if its star is disjoint from ∂S and every separatrix in the boundary of this star is typical.

LEMMA 6.7. *The number of deep vertex types is at most* $48n^2$.

Proof. Consider a deep vertex and all the vertices that are of the same type. Their stars are normally parallel. Consider the outermost stars in this collection. Transversely orient these so that they are both pointing away from the other stars of the same type. (If there is just one star in the collection, we consider it twice, with the two different transverse orientations.) By the definition of a deep vertex, these stars have only typical separatrices in their boundary. So, each such star is a union of elementary normal triangles, squares and half-squares. Since each of these stars is not normally parallel in the specified transverse direction to another star of the same type, we deduce that it contains an elementary normal triangle, square or half-square that is not parallel to another elementary normal triangle, square or half-square in the specified transverse direction. There are at most four triangle types and at most one square type in S in each truncated tetrahedron, and there are at most $4n^2$ truncated tetrahedra. Hence, there are at most $48n^2$ outermost triangles, squares or half-squares in the specified transverse direction. Each one of these outermost triangles, squares or half-squares that is in the star of a deep vertex lies in a single tile and therefore lies in the star of at most two vertices. This gives the upper bound. □

LEMMA 6.8. *The number of vertices of S that are not deep is at most $3288n^2$.*

Proof. Each vertex that is not deep lies in the boundary of a disc tile that is not ordinary. (Note that annular tiles are not incident to any vertices.) By Lemma 6.5, at most $1644n^2$ disc tiles are not ordinary. Each gives rise to two vertices that are not deep. □

6.9. *Poles.*

LEMMA 6.9. *Let S be the characteristic surface in normal* PL*-admissible form. Let $w_\beta(S)$ be the number of points of intersection between S and S^1_ϕ. Suppose that $(w_\beta(S), w(S))$ is minimal among all normal characteristic surfaces with boundary equal to ∂S. Then, S has at most $208n^2$ poles. Moreover, if S is closed, then in fact it contains no poles.*

Proof. Let p be a pole of the foliation. We claim that p has nonempty intersection with an elementary normal disc that is not a triangle or square. Now, the interior of each elementary triangle and square contains no poles. So, a pole that is only incident to triangles and squares must lie in the 2-skeleton of $\mathcal{P}$. By construction, it does not lie in the interior of a face of $\mathcal{T}$. In fact, near edges of $\mathcal{T} - (S^1_\theta \cup S^1_\phi)$, the foliation also has no singularities. Since only vertices of S lie on S^1_ϕ, we deduce that the pole p lies on S^1_θ. Let e be the edge of the triangulation containing p. Let B be the union of the tetrahedra incident to e. If a square is incident to p, then it contains a fibre ending on p,

and so p is not then a pole. Thus, p is only incident to triangles. The union of these triangles is a disc D properly embedded in B. It forms the link in B of one of the endpoints x of e. Let D' be the remainder of the link of x in $\mathcal{T}$. Note that D and D' have the same number of triangles, by the way that $\mathcal{T}$ is constructed. Remove D from S, and replace it with D'. Then perform a further small isotopy that makes the surface transverse to the 1-skeleton of $\mathcal{P}$. This leaves ∂S unchanged, and it also does not change $w_\beta(S)$. But it has decreased $w(S)$. By Theorems 5.1 or 5.2, there is a normal characteristic surface with the same boundary as S but smaller complexity. This is contrary to hypothesis, proving the claim.

So, consider an elementary normal disc that is not a triangle or square. There are at most $8n^2$ of these. By Lemma 6.2, it contains at most 24 poles in its interior. Any pole on its boundary lies on ∂S or S^1_θ. The elementary normal disc intersects S^1_θ at most once. So, the number of poles not lying on ∂S is at most $200n^2$. There are at most $8n^2$ poles lying on ∂S.

Note that the claim also implies that, when S is closed, it contains no poles. This is because S then consists only of triangles and squares. □

6.10. *Moves on* PL*-admissible surfaces.* Dynnikov's argument, described in Section 3, dealt with admissible surfaces. But many of these arguments work just as well with PL-admissible surfaces. For example, we have the following result.

PROPOSITION 6.10. *Let D be an arc presentation of a link L with arc index n. Let S be a* PL*-admissible surface properly embedded in the polyhedral decomposition $\mathcal{P}$.*

(1) *Suppose that S contains a deep 2-valent vertex. Then there is a generalised exchange move on the link, followed by an ambient isotopy of the link complement, taking S to a surface S' such that $w_\beta(S') \leq w_\beta(S) - 2$.*
(2) *Suppose that S contains a deep 3-valent vertex. Then there is a sequence of at most $n/2$ cyclic permutations, at most $n^2/4$ exchange moves, a generalised exchange move and some ambient isotopies on the link complement, taking S to a surface S' such that $w_\beta(S') \leq w_\beta(S) - 2$.*

Proof. (1) A picture of the star of a deep 2-valent vertex is shown in Figure 12. The saddles x_1 and x_2 shown there may be generalised saddles and so may have many separatrices emanating from them, but this does not affect the argument. The arrangement of the characteristic surface is shown in Figure 13, and one may make the same ambient isotopy that reduces the number of intersections with the binding circle by 2.

(2) A picture of the star of a deep 3-valent vertex is shown in Figure 15, but in the case where all generalised saddles are actual saddles. When x_1 and x_2 are generalised saddles, then there may be several vertices in Figure 15

between s_5 and s_2, and between s_6 and s_4, which are joined by separatrices to x_1 and x_2 respectively. But we can nevertheless perform the modification described in Figure 15 without involving these vertices. This requires at most $n/2$ cyclic permutations and at most $n^2/4$ exchange moves. It converts the deep 3-valent vertex into a deep 2-valent one. We then proceed as in (1). □

However, we require a stronger version of this, which involves many vertices at a time. This is absolutely central to this paper.

PROPOSITION 6.11. *Let D be an arc presentation of a link L with arc index n. Let S be a* PL*-admissible surface properly embedded in the polyhedral decomposition $\mathcal{P}$.*

(1) *Suppose that S contains m deep 2-valent vertices, all with normally parallel stars. Then there is a generalised exchange move followed by an ambient isotopy, taking S to a surface S' such that $w_\beta(S') \leq w_\beta(S) - 2m$.*
(2) *Suppose that S contains m deep 3-valent vertices, all with normally parallel stars. Then there is a sequence of at most $n/2$ cyclic permutations, at most $n^2/4$ exchange moves, a generalised exchange move and some ambient isotopies, taking S to a surface S' such that $w_\beta(S') \leq w_\beta(S) - 2m$.*

Proof. This follows the above argument. However, m copies of the surface shown in Figures 12 or 15 are used, all of which are parallel. Thus, in (1), once the generalised exchange move is performed, the ambient isotopy shown in Figure 14 can be applied, which reduces the number of intersections with S^1_ϕ by $2m$. The argument in (2) is similar. □

6.11. *Relating admissible and normal surfaces.* In this paper, we are considering four types of surface: admissible surfaces, alternative admissible surfaces, PL-admissible surfaces, and normal surfaces. It will be crucial to be able to pass between these different types of surface, as each will play an important role. In this subsection, we explain how to do this in one direction, while maintaining control of the complexity of the surfaces.

PROPOSITION 6.12. *Let D be an arc presentation for the unknot L with arc index n. Let S be a compression disc for $\partial N(L)$ in $S^3 - \mathrm{int}(N(L))$ that is in normal* PL*-admissible form with respect to $\mathcal{P}$. Suppose that ∂S is equal to the specified longitude and that its twisting number is t. Then there is a characteristic surface S' for L that is in admissible form such that $w_\beta(S') \leq w_\beta(S) + n$. Moreover, if S' contains a winding vertex, then its winding angle is at most $2\pi t$.*

Proof. Let $N(L)$ be the regular neighbourhood of L that is removed when forming $\mathcal{P}$. Let $N_-(L)$ be a much smaller regular neighbourhood of L. We initially set S' to equal S in $S^3 - \mathrm{int}(N(L))$.

When Dynnikov shows in [8] how a characteristic surface may be placed in admissible form, the first thing that he does is to arrange it near L so that it has the correct boundary behaviour. (See Section 3.1.) We do the same here, so that the characteristic surface S' lies in $N_-(L)$ in this specified way. It therefore picks up n intersection points with S^1_ϕ, which are precisely the vertices of the arc presentation.

We now need to explain how to arrange S' in $N(L) - N_-(L)$. Note that in this region, there lie the arcs $S^1_\phi \cap (N(L) - N_-(L))$, which are vertical in its product structure. We need to ensure that S' has no intersection points with these arcs. Then the binding weight of S', which is just the number of intersection points with S^1_ϕ, is $w_\beta(S) + n$.

Now, the two curves $S \cap \partial N(L)$ and $S' \cap \partial N_-(L)$ are already fixed. Using the product structure on $\mathrm{cl}(N(L) - N_-(L))$, we may identify $\partial N(L)$ and $\partial N_-(L)$ and, therefore, view these two curves as lying on the same torus. The former curve is equal to the specified longitude, and the latter is arranged according to the recipe given by Dynnikov, as described in Section 3.1. But the specified longitude is defined precisely so that these are equal, up to an ambient isotopy in the complement of S^1_ϕ. Thus, there is a way of inserting S' into this product region, so that it is an annulus interpolating between these two curves, and without introducing any new intersection points with S^1_ϕ.

Note that S', as constructed, is piecewise-linear, not smooth. Also, its singularities are poles and generalised saddles. But a small ambient isotopy, supported away from $N_-(L)$, makes S' smooth with Morse-type singularities. This does not change its binding weight, and it turns S' into an admissible surface.

In the definition of the specified longitude in Section 6.4, a normal curve C' was first defined. The specified longitude was obtained from C' by performing t Dehn twists along a meridian of L. This is the location for a winding vertex of S' (if it has one). By construction, its winding angle is therefore at most $2\pi t$. □

7. The Euler characteristic argument

THEOREM 7.1. *Let L be the unknot or a split link. Fix an arc presentation of L with arc index n that is not disconnected. Let S be a characteristic surface in* PL*-admissible normal form with respect to the polyhedral decomposition $\mathcal{P}$, as described in Section* 6.5. *Suppose that S is a boundary-vertex surface. In the case where L is the unknot, suppose also that ∂S is the specified longitude. Let $w_\beta(S)$ be the number of points in $S \cap S^1_\phi$, and let $w(S)$ be the weight of S. Suppose that $(w_\beta(S), w(S))$ is minimal among all characteristic surfaces with the same boundary as S. Then, the number of deep* 2*-valent and* 3*-valent*

vertices is at least

$$\frac{w_\beta(S)}{2 \times 10^9 n^4} - 4833n^2.$$

Moreover, if L is a split link and hence S is closed, the number of such vertices is at least

$$\frac{w_\beta(S)}{2 \times 10^9 n^4}.$$

We now define a Euclidean subsurface of S, which will play a key role in the proof. The *designated Euclidean subsurface* E of S is obtained as follows. It includes the interiors of the ordinary tiles. If two such tiles are adjacent along a separatrix, add the interior of this separatrix. If a vertex is 4-valent and is completely surrounded by ordinary tiles, add it in. Similarly, if a saddle is completely surrounded by ordinary tiles, add it in.

We now give E a Riemannian metric that is locally isometric to the Euclidean plane. Each ordinary tile has, by definition, only typical separatrices in its boundary, each of which runs between a vertex of S and a generalised saddle. So it has precisely four separatrices in its boundary (as in the left of Figure 11). We realise it as the interior of a Euclidean square with side length 1. When the interiors of edges are added, they are realised as Euclidean geodesics with length 1. The Euclidean metric extends over the vertices and saddles that are added to form E, in a natural way.

Denote the *combinatorial length* $\ell(\partial E)$ of ∂E to be the number of separatrices in ∂E plus the number of components of ∂E that are isolated points.

LEMMA 7.2. *Suppose that each point of E is at a distance at most R from ∂E. Then, the area of E is at most $\pi(R+1)^2\ \ell(\partial E)$.*

Proof. For each point y in E, there is a shortest path from y to ∂E, which is a Euclidean geodesic. Let x be the endpoint of this geodesic in ∂E. Then y lies in the image of the exponential map based at x. Call this map $\exp_x$. It is defined on a star-shaped subset of T_xE centred at the origin, which we denote by $\mathrm{dom}(\exp_x)$. In fact, if we set $S(R,x)$ to be $\exp_x(B(R,0) \cap \mathrm{dom}(\exp_x))$, then y lies in $S(R,x)$. Thus, we have shown that E equals $\bigcup_{x \in \partial E} S(R,x)$.

We now show in fact that E equals the union of $S(R+1,x)$, as x runs over all 0-cells in ∂E. By a 0-cell, we mean a corner of one of the tiles, which may be a generalised saddle or vertex of $\mathcal{F}$. For suppose that α is a shortest geodesic joining y to ∂E and that its endpoint x is in the interior of a side of one of the tiles. Then α is orthogonal to this side. So, if we slide x to one of the endpoints x' of this side, keeping α a geodesic, then it remains in the same set of tiles. In particular, it remains in E. This process increases the length of α by at most 1. So, y lies in $S(R+1,x')$.

Now, $\exp_x$ is a local isometry from $B(R+1,0)\cap\mathrm{dom}(\exp_x)$ onto $S(R+1,x)$. Hence, the area of $S(R+1,x)$ is at most $\pi(R+1)^2$. So, the area of E is at most $\ell(\partial E)$ times the maximal area of $S(R+1,x)$, which gives the required bound. □

The proof of the following key result will take up the entirety of Section 9.

THEOREM 7.3. *Let L, n and S be as in Theorem* 7.1. *Let E be the designated Euclidean subsurface of the characteristic surface S. Then each point of E has distance at most $8000n^2$ from ∂E.*

Proof of Theorem 7.1. Let Γ be the following 1-complex embedded in S. Its 1-cells are the separatrices. Its 0-cells are the endpoints of these separatrices, plus the poles. This includes the vertices of S, the generalised saddles and the endpoints of separatrices on ∂S.

Let S_+ be two copies of S glued along ∂S via the identity map. (So, when S is a sphere, S_+ is two 2-spheres.) So, $\chi(S_+)\geq 2$. Let Γ_+ be the union of the copies of Γ in S_+. Then, $S_+-\Gamma_+$ is a collection of open annuli and discs. Let S_- be the result of removing the open annuli from S_+. Then $\chi(S_-)=\chi(S_+)\geq 2$.

Now, S_- inherits a cell structure. When a separatrix in S ends at a nonsingular point on ∂S, then combine the two copies of this separatrix in S_- into a single 1-cell. So, each 0-cell of S_- comes from a vertex, pole or generalised saddle of $\mathcal{F}$. For $i=0$, 1 and 2, let S_-^i denote the i-cells of S_-. For each 0-cell v, let $d(v)$ denote its valence.

Each 2-cell of S_- has precisely four 1-cells in its boundary that are not loops. Hence, $2|S_-^1|\geq 4|S_-^2|$. Therefore,

$$2\leq\chi(S_-)=|S_-^0|-|S_-^1|+|S_-^2|\leq|S_-^0|-|S_-^1|/2=\sum_{v\in S_-^0}(1-d(v)/4).$$

Let V denote the set of vertices of S, let P denote the set of poles of S and let X denote the set of generalised saddles in the interior of S. The boundary-saddles give rise to 0-cells of S_- with valence 4, and so they do not contribute to the above summation. Therefore,

$$2\leq\sum_{v\in S_-^0}(1-d(v)/4)=2|P|+2\sum_{v\in V}(1-d(v)/4)+2\sum_{x\in X}(1-d(x)/4).$$

For $k\geq 2$, let v_k denote the number of vertices in S with valence k. Note that there are no vertices of valence 1 in the interior of S, as explained in the proof of Lemma 5 in [8]. Note also that $|P|\leq 208n^2$, by Lemma 6.9. Moreover, $|P|$ is zero when S is closed. So, $|P|\leq 208n^2|\partial S|$. So,

$$2v_2+v_3=\sum_{\substack{v\in V\\ d(v)<4}}(4-d(v))\geq 4+\sum_{\substack{v\in V\\ d(v)>4}}(d(v)-4)+\sum_{x\in X}(d(x)-4)-832n^2|\partial S|.$$

Note that

$$\sum_{\substack{v\in V\\ d(v)>4}} (d(v)-4) = \sum_{k>4} \sum_{\substack{v\in V\\ d(v)=k}} (d(v)-4) = \sum_{k>4} v_k(k-4) \geq \sum_{k>4} v_k.$$

Similarly, because each generalised saddle in the interior of S has even valence at least 4, we deduce that

$$\sum_{x\in X} (d(x)-4) \geq \frac{1}{3} \sum_{\substack{x\in X\\ d(x)\neq 4}} d(x).$$

So,

$$2v_2 + v_3 > \frac{1}{3}\left(3\sum_{k>4} v_k + \sum_{\substack{x\in X\\ d(x)\neq 4}} d(x) \right) - 832n^2|\partial S|. \tag{1}$$

Let v_4^E be the vertices lying in the interior of E, each of which is 4-valent by construction. Let v_4^{NE} denote the number of remaining 4-valent vertices. Each of the vertices in the interior of E contributes 1 to the area of E. So, by Lemma 7.2 and Theorem 7.3,

$$v_4^E \leq \pi(8000n^2+1)^2\ \ell(\partial E).$$

So,

$$v_4 = v_4^E + v_4^{NE} \leq \pi(8000n^2+1)^2\ \ell(\partial E) + v_4^{NE} \leq \pi(8000n^2+1)^2(\ell(\partial E) + v_4^{NE}).$$

Each fibre in ∂E is adjacent to a disc tile that is not ordinary. The number of such tiles is at most $1644n^2|\partial S|$, by Lemma 6.5. Each contributes at most 4 to $\ell(\partial E)$. Each isolated point of ∂E is a generalised saddle with valence not equal to 4 or a vertex with valence not equal to 4. Each 4-valent vertex not in the interior of E is adjacent to a disc tile that is not ordinary. This tile contributes at most 2 to v_4^{NE}. So, we deduce that

$$\ell(\partial E) + v_4^{NE} \leq 9864n^2|\partial S| + \sum_{k\neq 4} v_k + \sum_{\substack{x\in X\\ d(x)\neq 4}} d(x).$$

Therefore,

$$\begin{aligned} v_2 + v_3 &\geq \ell(\partial E) + v_4^{NE} - \sum_{k>4} v_k - \sum_{\substack{x\in X\\ d(x)\neq 4}} d(x) - 9864n^2|\partial S| \\ &\geq \frac{v_4}{\pi(8000n^2+1)^2} - \sum_{k>4} v_k - \sum_{\substack{x\in X\\ d(x)\neq 4}} d(x) - 9864n^2|\partial S|. \end{aligned} \tag{2}$$

Adding three times (1) to (2), we deduce that

$$7v_2 + 4v_3 > \frac{v_4}{\pi(8000n^2+1)^2} + 2\sum_{k>4} v_k - 12360n^2|\partial S|.$$

Therefore,

$$\begin{aligned} 8v_2 + 5v_3 &> \frac{v_4}{\pi(8000n^2+1)^2} + \sum_{k\neq 4} v_k - 12360n^2|\partial S| \\ &> \frac{|V|}{\pi(8000n^2+1)^2} - 12360n^2|\partial S|. \end{aligned}$$

The next stage is to discard vertices that are not deep. By Lemma 6.8, the number of these is at most $3288n^2|\partial S|$. Therefore, the number of deep 2-valent and 3-valent vertices in S is at least

$$\begin{aligned} v_2 + v_3 - 3288n^2|\partial S| &\geq \frac{8v_2+5v_3}{8} - (3288n^2|\partial S|) \\ &\geq \frac{w_\beta(S)}{8\pi(8000n^2+1)^2} - 4833n^2|\partial S| \\ &\geq \frac{w_\beta(S)}{2\times 10^9 n^4} - 4833n^2|\partial S|, \end{aligned}$$

as required. □

We are now in a position to prove Theorems 1.4 and 1.3, assuming Theorem 7.3.

Proof of Theorem 1.4. Let D be an arc presentation of a split link L. Suppose that D is not disconnected. Let n be its arc index. Let $\mathcal{T}$ denote Dynnikov's triangulation of S^3, given in Section 6.1. By Theorem 5.1, there is a splitting 2-sphere for $S^3 - L$ that is in normal form with respect to $\mathcal{T}$. By Theorem 5.5, there is such a sphere S that is a vertex surface with respect to $\mathcal{T}$, for which $(w_\beta(S), w(S))$ is minimal. By Theorem 5.9, the binding weight $w_\beta(S)$ of this surface is at most $n2^{7n^2}$, which is less than 2^{8n^2}. The surface S inherits a singular foliation. Then by Theorem 7.1, the number of 2-valent and 3-valent vertices in S is at least

$$\frac{w_\beta(S)}{2\times 10^9 n^4}.$$

By Lemma 6.7, these vertices come in at most $48n^2$ types. So, there is a collection of at least $w_\beta(S)/(10^{11}n^6)$ 2-valent or 3-valent vertices, all of the same type. Applying Proposition 6.11, there is a sequence of at most $n/2$ cyclic permutations, at most $n^2/4$ exchange moves, a generalised exchange move and some ambient isotopies, which reduces the binding weight of the surface by at least $2w_\beta(S)/(10^{11}n^6)$.

After we have performed these moves, the result is a new arc presentation of L. This gives a new triangulation, which we will call $\mathcal{T}'$. Now, the

new surface S' need not be normal, but by Theorem 5.1, there is reducing 2-sphere that is normal with respect to $\mathcal{T}'$ and with no greater binding weight. We may therefore repeat the above argument with this new arc presentation, triangulation and splitting sphere.

Let x be the number of these steps required to reduce the complexity down to less than 1, by which time we must have reach a disconnected arc presentation, as required. Then

$$2^{8n^2}\left(1-\frac{2}{10^{11}n^6}\right)^{x-1} \geq 1,$$

because after $x-1$ steps, the binding weight is still at least 1, by the definition of x. Taking logs, we obtain

$$(x-1)\log\left(1-\frac{2}{10^{11}n^6}\right)+8n^2\log 2 \geq 0.$$

Now, $\log(1-y) \leq -y$ for any y between 0 and 1, and so

$$(x-1) \leq (8n^2\log 2)(10^{11}n^6/2).$$

Therefore $x \leq 3\times 10^{11}n^8$, which proves the theorem. □

Proof of Theorem 1.3. We now consider the case where L is the unknot. The argument is similar to that of Theorem 1.4, but it is made more complicated by the presence of boundary. A flowchart for the proof is shown in Figure 25.

Let M be the exterior of L, and let $\mathcal{P}$ be the polyhedral structure for M defined in Section 6.2. Let C be the specified longitude. Now apply Theorem 5.2 to find a compression disc S for ∂M that is normal and with boundary equal to C. By Theorem 5.6, we may choose S so that it is a boundary-vertex surface and so that $(w_\beta(S), w(S))$ is minimal. So, by Theorem 5.10 and Lemma 6.1, its binding weight $w_\beta(S)$ is at most

$$(2n)(2\times 10^6)^{4\times 10^6 n^2}(8n^2) < 2^{10^8 n^2}.$$

Now suppose that $w_\beta(S) > 2\times 10^{13}n^6$. Then by Theorem 7.1, the number of deep 2-valent and 3-valent vertices in S is at least

$$\frac{w_\beta(S)}{2\times 10^9 n^4} - 4833n^2 \geq \frac{w_\beta(S)}{4\times 10^9 n^4}.$$

By Lemma 6.7, these vertices come in at most $48n^2$ types. So, there is a collection of at least $w_\beta(S)/(2\times 10^{11}n^6)$ deep 2-valent or 3-valent vertices, all of the same type. By Proposition 6.11, we may perform at most $n/2$ cyclic permutations, at most $n^2/4$ exchange moves, a generalised exchange move and some ambient isotopies, to reduce the binding weight by at least $w_\beta(S)/(10^{11}n^6)$.

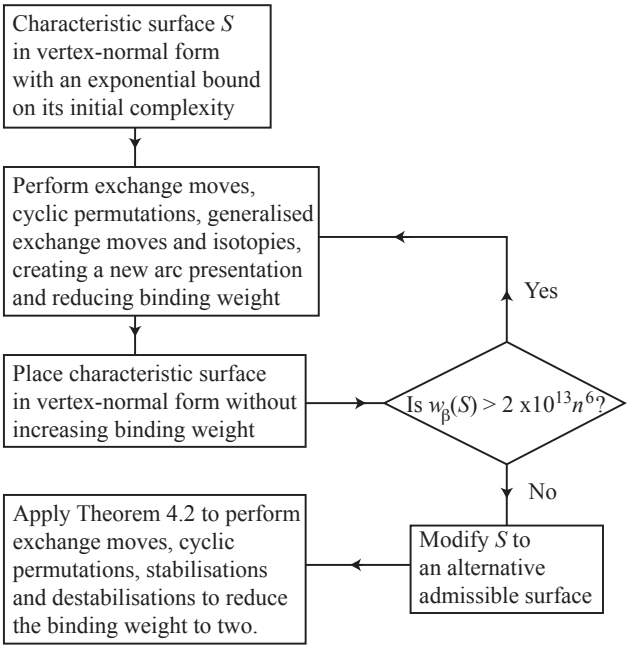

Figure 25. Flowchart for the proof of Theorem 1.3

As in the proof of Theorem 1.4, this creates a new arc presentation of L. This then gives a new polyhedral decomposition $\mathcal{P}'$. Let S' be the result of S after making this modification. Then, S' is a surface properly embedded in the exterior of the new copy of L. Its boundary remains a longitude on $\partial N(L)$. Moreover, the decomposition of L into 'up' and 'down' arcs, plus possibly one extra arc, is preserved. And near these arcs, S' continues to lie in the up and down directions from L. We may therefore isotope $\partial S'$, taking it to the new specified longitude for L, without changing its binding weight. By Theorem 5.6, there exists a normal disc S'' in $\mathcal{P}'$ with boundary this specified longitude that is a boundary-vertex surface, such that $w_\beta(S'') \leq w_\beta(S')$. We choose S'' so that $(w_\beta(S''), w(S''))$ is minimal. We then repeat the above argument.

Let x be the number of steps required to reduce the complexity down to at most $2 \times 10^{13} n^6$. By the above argument,

$$x \leq (10^8 n^2 \log 2)(10^{11} n^6) + 1 \leq 10^{19}\, n^8.$$

This is at most $3 \times 10^{18} n^{10}$ exchange moves, at most $5 \times 10^{18} n^9$ cyclic permutations and at most $10^{19} n^8$ generalised exchange moves. Once we have reduced the binding weight below $2 \times 10^{13} n^6$, we apply Proposition 6.12 to create a characteristic surface in admissible form with binding weight at most $2 \times 10^{13} n^6 + n$. If it has a winding vertex, its winding angle is at most 2π times the twisting

number of the specified longitude. Now, the exchange moves, cyclic permutations and generalised exchange moves that we have performed so far do not affect the writhe of the rectangular diagram, which therefore remains k. So, as explained in Section 6.4, the twisting number of the specified longitude is at most $|k|+n+1$. So, by Lemma 4.1, there is a sequence of at most $|k|+n < n^2$ stabilisations, less than $n^2(n+n^2)$ exchange moves and an ambient isotopy of the knot complement taking the characteristic surface into alternative admissible form with binding weight at most $2 \times 10^{13} n^6 + n + n^2$. Then, by Theorem 4.2, there is a sequence of at most $4(n+n^2)^2(2 \times 10^{13} n^6 + n + n^2)$ exchange moves, at most $(n+n^2)(2 \times 10^{13} n^6 + n + n^2)$ cyclic permutations, at most $(2 \times 10^{13} n^6 + n + n^2)$ stabilisations and at most $(2 \times 10^{13} n^6 + n + n^2)$ destabilisations taking D to the trivial arc presentation. So, the total number of exchange moves is at most

$$(3 \times 10^{18}) n^{10} + n^2(n+n^2) + 4(n+n^2)^2(2 \times 10^{13} n^6 + n + n^2) \leq 4 \times 10^{18} n^{10}.$$

The total number of cyclic permutations is at most

$$(5 \times 10^{18}) n^9 + (n+n^2)(2 \times 10^{13} n^6 + n + n^2) \leq 6 \times 10^{18} n^9.$$

The number of stabilisations and destabilisations are each at most

$$n^2 + (2 \times 10^{13} n^6 + n + n^2) \leq 3 \times 10^{13} n^6,$$

as required. □

8. **Branched surfaces**

The remainder of this paper is devoted to the proof of Theorem 7.3. The proof will be given in Section 9, but it requires some background theory on branched surfaces, which we recall in this section. This is mostly standard material, which can be found, for example, in [9].

8.1. *Definitions.* A *branched surface* is a compact 2-complex B smoothly embedded in a 3-manifold M, with the following properties. At each point x of B, there is a specified tangent plane in $T_x(M)$ and all the 1-cells and 2-cells that contain x have tangent spaces at x that lie in this tangent plane. This tangent plane is denoted by $T_x(B)$. Thus, at each point x in the interior of a 1-cell of B, $T_x(B)$ is divided into two half-planes by the tangent space of the 1-cell. We term these the two *sides* at x. We require that, at each such point x, either there are 2-cells on both sides of x or the 1-cell is incident to a single 2-cell. The closure of the union of the points x of the former type is the *branching locus* of B. The closure of the union of the points x of the latter type is the *boundary* of B, which we denote by ∂B. (Note that we do not require ∂B to lie in ∂M.) The 2-cells of B are called the *patches* of B.

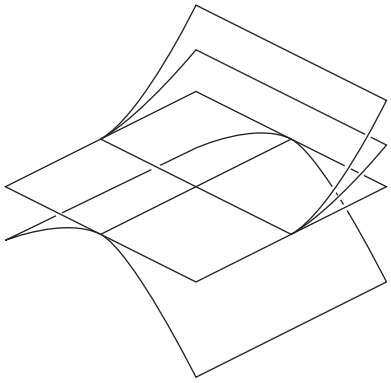

Figure 26. A branched surface

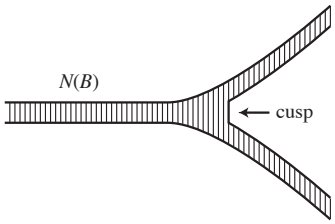

Figure 27. The fibred neighbourhood of B

Note that this definition is somewhat more general than the one that is frequently used, for example, in [9]. There, a branched surface is defined via its possible local models. In our definition, it is not the case that there are only finitely many local models. An example is shown in Figure 26, but this is not the general situation.

A thickening $N(B)$ of B has a decomposition as a union of *fibres*, each of which is homeomorphic to an interval. (This thickening is almost a regular neighbourhood, except that $\partial B \subset \partial N(B)$.) Away from a small regular neighbourhood of the 1-skeleton of B, this is just an I-bundle. There is a map $\pi\colon N(B) \to B$ that collapses each fibre to a point. For each $x \in B$, the fibre through x is required to have tangent space that is complementary to $T_x(B)$. Also, each fibre is required to intersect $\partial N(B)$ in its endpoints, plus possibly a finite collection of closed intervals (see Figure 27). The *horizontal boundary* $\partial_h N(B)$ is the union of the endpoints of these fibres. The *vertical boundary* $\partial_v N(B)$ is $\mathrm{cl}(\partial N(B) - \partial_h N(B))$. Each component of $\mathrm{cl}(\partial_v N(B) - \pi^{-1}(\partial B))$ is termed a *cusp*.

Due to the potential interaction between ∂B and the branching locus, these cusps can have slightly complicated topology. However, in the following case, they are rather simple.

LEMMA 8.1. *Let B be a branched surface in an orientable 3-manifold M. Suppose that $B \cap \partial M = \partial B$ and that $\pi^{-1}(\partial B) = N(B) \cap \partial M$. Suppose also that at each $x \in \partial B$, the tangent plane $T_x(B)$ does not equal $T_x(\partial M)$. Then each cusp either is an annulus or is a disc D such that $D \cap \partial M$ is two disjoint arcs in ∂D.*

Proof. The cusps lie in a regular neighbourhood of the 1-skeleton of B. Near each 1-cell of B, they have a simple form. They have the structure of I-bundles over this 1-cell, where each I-fibre is the intersection between the cusp and a fibre of $N(B)$. We need to analyse how these I-bundles join together near the 0-cells of B. We claim they patch together to give each cusp the structure of an I-bundle.

Let v be a 0-cell of B in the interior of M. Pick a small smoothly embedded disc P running through v with tangent plane at v equal to $T_v(B)$. Let N be a thickening of P, which is an I-bundle over P, and let A be the I-bundle over ∂P, which is an annulus in ∂N. Then we may arrange that $B \cap \partial N$ lies in the interior of A and that it is transverse to the I-fibres of A. It is a branched 1-manifold in A. By our hypothesis on ∂B, this branched 1-manifold has no boundary. Hence, it divides A into a collection of bigons, together with at least two annuli with smooth boundary. At each such bigon, two cusps of $N(B)$ enter and are joined together. We deduce that the I-bundle structures do indeed patch together correctly here.

A similar analysis applies near each 0-cell v of B that lies in ∂M. Again, pick a small smoothly embedded disc P that contains v, and with tangent plane at v that equals $T_v(B)$. Then P may be chosen so that $P \cap \partial M$ is a single arc in ∂P that contains v in its interior. Thicken P to an I-bundle N over ∂P. Let W be the I-bundle over $\mathrm{cl}(\partial P - \partial M)$, which is a disc. Again, we may assume that $B \cap W$ is transverse to the fibres. It therefore divides W into a collection of bigons, at least two smooth discs that include collars on the horizontal boundary of W, and some discs, each of which has a single cusp in its boundary and a single arc of intersection with ∂W. At this latter type of disc, a cusp of $N(B)$ hits ∂M and terminates. At each bigon, two bits of cusp of $N(B)$ join together. Thus, again, we deduce that I-bundle structures patch together as required, proving the claim.

Since each cusp lies in the boundary of the orientable 3-manifold $N(B)$, we deduce that it is orientable and hence an annulus or disc, as required. □

8.2. *Surfaces carried by branched surfaces.* A compact surface S is *carried* by a branched surface B if S is embedded in $N(B)$, it is transverse to the fibres and $S \cap \pi^{-1}(\partial B) = \partial S$. These conditions ensure that, for each patch of B, the cardinality of $\pi^{-1}(x) \cap S$ is constant for all x in the interior of that patch. This cardinality is termed the *weight* of S in that patch. These weights form

a collection of nonnegative integers, which is known as the *vector* associated with S, and is denoted by $[S]$. The weights satisfy a system of linear equations, which are known as the *matching equations*. These specify that, at each 1-cell in the branching locus of B, the total weight of the patches on one side is equal to the total weight of the patches on the other. Conversely, given a solution to these matching equations by nonnegative integers, one can form a compact surface carried by B with these weights.

8.3. *Summation of surfaces.* Let S, S_1 and S_2 be surfaces carried by B. Then S is said to be the *sum* of S_1 and S_2 if $[S] = [S_1] + [S_2]$. We say that S_1 and S_2 are *summands* of S.

There is an alternative way of viewing summands of a surface.

LEMMA 8.2. *Let S and S_1 be surfaces carried by a branched surface B. Then S_1 is a summand of S if and only if, in every patch of B, the weight of S is at least the weight of S_1.*

Proof. Suppose that S and S_1 satisfy this weight condition. Consider the vector $[S] - [S_1]$. Since $[S]$ and $[S_1]$ satisfy the matching equations, so does $[S] - [S_1]$. By assumption, each of its co-ordinates is nonnegative. Hence, it corresponds to a surface S_2 carried by B, and S is the sum of S_1 and S_2.

Conversely, if S is the sum of S_1 and S_2, then clearly, the weight of S is at least the weight of S_1 in each patch. □

8.4. *Branched surfaces associated to normal surfaces.* Let $\mathcal{P}$ be a polyhedral decomposition of a compact 3-manifold M. Associated to any normal, properly embedded surface S, there is a branched surface B_S, which we term a *normal* branched surface. It carries S.

It is constructed as follows. For each type of elementary normal disc in S, we take one such disc. We arrange for these discs to be smoothly embedded. They form the patches of B_S. For each face F of $\mathcal{P}$ with polyhedra on both sides and for each arc type of $F \cap S$, we glue all patches of B_S that contain this arc type along this arc.

This is a branched surface, because the tangent planes to B_S can be defined as follows. For each $x \in B_S$ lying in a 1-cell of $\mathcal{P}$, pick a tangent plane $T_x(B_S)$ that does not contain the tangent plane of the 1-cell. For each $x \in B_S$ lying in the interior of a face of $\mathcal{P}$, pick a tangent plane not equal to the tangent plane of the face. We can do this compatibly with the choices for the points in the 1-cells of $\mathcal{P}$. For each point x inside the interior of a patch, we define $T_x(B_S)$ to be the tangent plane of the elementary normal disc in which it lies. Although no Riemannian metric has been specified, one should still think of the tangent planes of B_S at the 1-cells and 2-cells of $\mathcal{P}$ as being 'orthogonal' to those cells.

Note that S is carried by B_S. For we may take a regular neighbourhood $N(S)$ of S, such that $N(S)$ intersects each polyhedron in a union of elementary normal discs. Then, when two elementary normal discs of S are normally parallel, we attach the space between them to $N(S)$. Also, when two arcs of S in a face of $\mathcal{P}$ are normally parallel, we attach a slight thickening of the space between them to $N(S)$. The resulting space is a 3-dimensional subset of the 3-manifold, which we term $N(B_S)$. It is composed of a collection of regions, each of which is the product of an elementary normal disc type of S with an interval. There is therefore a map $\pi\colon N(B_S) \to B_S$ that collapses these intervals to points. It is clear that $N(B_S)$ is a fibred regular neighbourhood of B_S. By construction, S is a subset of $N(B_S)$ that is transverse to the fibres. The boundary of B_S is precisely $B_S \cap \partial M$. So, $\pi^{-1}(\partial B_S) \cap S = S \cap \partial M = \partial S$.

When a surface S' is carried by B_S, it is normal with respect to $\mathcal{P}$. Moreover, the vector for S' as a surface carried by B_S is equal to its normal surface vector. Hence, summation of surfaces in the branched surface B_S corresponds to the summation of normal surfaces. More precisely, suppose that S', S_1 and S_2 are surfaces carried by B_S such that S' is the sum of S_1 and S_2. Then these are normal and $S' = S_1 + S_2$ as normal surfaces. Conversely, if S, S_1 and S_2 are normal surfaces satisfying $S = S_1 + S_2$, then, when one forms the branched surface B_S starting from the normal surface S, then S, S_1 and S_2 are all carried by B_S and S is the sum of S_1 and S_2 in B_S.

8.5. *Branched surfaces carried by branched surfaces.* We say a branched surface B_1 is *carried* by a branched surface B_2 if

(1) B_1 is smoothly embedded in $N(B_2)$; and
(2) for each point x in B_1, $T_x B_1$ is transverse to the fibres of $N(B_2)$.

We do not require that ∂B_1 lies in $\pi^{-1}(\partial B_2)$, where $\pi\colon N(B_2) \to B_2$ is the collapsing map for B_2. In fact, $\pi(\partial B_1)$ is permitted to run through the interior of patches of B_2.

LEMMA 8.3. *If B_1 is carried by B_2, then any closed surface carried by B_1 is also carried by B_2.*

Proof. Let S be a closed surface carried by B_1. We may assume that, at each point of x of S, $T_x(S)$ is arbitrarily close to the tangent plane $T_{\pi(x)}(B_1)$, where $\pi\colon N(B_1) \to B_1$ is the collapsing map for B_1. Since $T_{\pi(x)}(B_1)$ is transverse to the fibre of $N(B_2)$ through $\pi(x)$, we can therefore arrange that $T_x(S)$ is also transverse to the fibre of $N(B_2)$ through x. For a closed surface, this is the definition of S being carried by B_2. □

9. **Euclidean subsurfaces of the characteristic surface**

This section is devoted to the proof of Theorem 7.3.

THEOREM 7.3 *Let L be the unknot or a split link. Fix an arc presentation of L with arc index n. Let S be a characteristic surface in* PL*-admissible normal form with respect to the polyhedral decomposition $\mathcal{P}$ and that is a boundary-vertex surface. In the case where L is the unknot, suppose that ∂S is the specified longitude. Suppose also that $(w_\beta(S), w(S))$ is minimal among all characteristic surfaces for L with the same boundary as S. Let E be the designated Euclidean subsurface of S. Then each point of E has distance at most $8000n^2$ from ∂E.*

For a subset F of a metric space and a positive real number r, let $N_r(F)$ denote the set of points with distance at most r from F. Thus, in our situation, Theorem 7.3 asserts that in the metric space E, $N_{8000n^2}(\partial E)$ is all of E.

9.1. *Overview of the proof.* The strategy for the proof is as follows. Suppose that there is a point in E with distance more than $8000n^2$ from ∂E. Then, around this point, there is a large Euclidean region. We will show that this implies that there is a normal torus that is a summand for some multiple of S. This will imply that S is not a boundary-vertex surface, which is contrary to hypothesis.

Throughout this section, S will be a characteristic surface for L that is in normal form with respect to the polyhedral decomposition, and that is a boundary-vertex surface. Also, $(w_\beta(S), w(S))$ is minimal among all characteristic surfaces for L with the same boundary as S. As above, E will denote the designated Euclidean subsurface of S. We will prove Theorem 7.3 by contradiction and therefore suppose that there is some point z in E with distance more than $8000n^2$ from ∂E. Let E' denote the component of E containing z.

9.2. *A branched surface carrying the Euclidean subsurface.* Starting with the designated Euclidean subsurface E, we can form a branched surface B as follows. By construction, E is a union of square-shaped tiles. We say that two tiles of E are *normally parallel* if they are normally parallel in $\mathcal{P}$. We first form a 2-complex $\overline{B}$, where each 2-cell of $\overline{B}$ arises from a normal equivalence class of tiles of E. Each 2-cell therefore has the shape of a square tile. We call each of these 2-cells a *Euclidean patch*. When two tiles of E are incident along a separatrix, then we glue the associated patches of $\overline{B}$ along the corresponding edges.

However, $\overline{B}$ is not quite a branched surface, because there may be 1-cells of $\overline{B}$ with more than one 2-cell on one side but no 2-cells on the other. To remedy this, we attach to $\overline{B}$ some extra 2-cells, as follows. For each normal equivalence class of tile T of S that is incident to E but not a subset of E, we attach a thin neighbourhood of $T \cap \partial E$. This is a collection of thin discs. The boundary of each such disc consists of two long arcs and two short arcs. When two such discs are incident because they share a common isotopy class of short

arc in their boundary, we glue these discs together along this arc, forming new branching locus on their boundary. The result is the branched surface B.

Note that we make no identifications on the long arcs that do not lie in ∂E. Instead, they become part of the boundary of B.

Note also that there is a retraction map $B \to \overline{B}$ that collapses the thin discs attached to $\overline{B}$. This is a homotopy equivalence.

LEMMA 9.1. *The number of Euclidean patches of B is at most $24n^2$.*

Proof. Each Euclidean patch of B corresponds to a normal isotopy class of ordinary tiles. These tiles are all normally parallel, and so there are two that are outermost, T_1 and T_2 say. We claim that each of T_1 and T_2 must contain an elementary normal triangle, square or half-square that is outermost in $N(B_S)$. Suppose that this is not the case, for T_1, say. Then, adjacent to each elementary normal triangle, square or half-square in T_1 on both sides of T_1, there is another elementary normal triangle, square or half-square and the union of these forms two tiles that are normally parallel to T_1 on both sides of T_1. These are ordinary tiles, which contradicts the assumption that T_1 is outermost in $N(B)$. This proves the claim.

As a consequence of the claim, the number of Euclidean patches of B is at most the number of normal isotopy classes of triangles, squares and half-squares in S. There are at most six of these in each truncated tetrahedron. There are at most $4n^2$ truncated tetrahedra in the polyhedral decomposition. This proves the lemma. □

LEMMA 9.2. *B is carried by B_S.*

Proof. We need to find an embedding $B \to N(B_S)$. Each Euclidean patch of B is a normal equivalence class of Euclidean tiles. The remaining patches are subsets of tiles. Each tile is made up pieces of elementary normal discs. Embed B into $N(B_S)$ by including each such piece into a regular neighbourhood of the relevant patch of B_S. It is easy to see that this inclusion map has the right properties. □

Let B' be the component of B such that $N(B')$ contains E'. Let $\overline{B}'$ be the component of $\overline{B}$ such that $N(\overline{B}')$ contains E'. Then the retraction map $B' \to \overline{B}'$ is a homotopy equivalence, using which we may identify $\pi_1(B')$ and $\pi_1(\overline{B}')$.

Note that E' is not carried by B', because we added non-Euclidean patches to $\overline{B}'$. But we can take a small regular neighbourhood of E' in S, denoted $\hat{E}$, so that $\hat{E}$ is carried by B'.

9.3. *Reducing to the case of trivial monodromy.* We now define a homomorphism $\mu\colon \pi_1(B') \to O(2)$, where $O(2)$ is the group of orthogonal transformations of $\mathbb{R}^2$. We term this the *monodromy* of the branched surface B'.

It is convenient to subdivide the cell structure on $\overline{B}'$, introducing a new vertex into the midpoint of each 1-cell of $\overline{B}'$, and introducing a new vertex in the centre of each 2-cell and coning off from this vertex. Let b be a basepoint for $\overline{B}'$, which is a vertex at the centre of one of the original 2-cells.

Around each vertex of this new cell structure, we pick a Euclidean disc of radius 1/4, say, that lies in B'. Given two vertices that are the endpoints of a 1-cell of $\overline{B}'$, there is a canonical isometry taking one disc to the other, which is Euclidean translation along the 1-cell. If one follows a loop that encircles a 2-cell of $\overline{B}'$, the composition of these Euclidean isometries is the identity. Thus, one may define $\mu\colon \pi_1(\overline{B}') \to O(2)$ as follows. Given a cellular loop ℓ in $\overline{B}'$ based at b, it is a composition of paths along 1-cells, and this then gives a composition of Euclidean isometries. This composition is a Euclidean isometry that takes the disc neighbourhood of b to itself. It is therefore an element of the orthogonal group $O(2)$. Because the monodromy around each 2-cell is trivial, this gives a well-defined homomorphism $\mu\colon \pi_1(\overline{B}') \to O(2)$ and hence a homomorphism $\mu\colon \pi_1(B') \to O(2)$. Note that $\mu(\ell)$ is an isometry that preserves the tile containing b, and hence the image of μ lies in a subgroup of $O(2)$ of order 8.

We now define a finite-sheeted cover $\tilde{B}$ of B', as follows. We let $\tilde{B}$ be the covering space of B' corresponding to kernel of the monodromy homomorphism $\mu\colon \pi_1(B') \to O(2)$.

We record some properties of $\tilde{B}$.

PROPERTY 9.3. *$\tilde{B}$ is a branched surface.*

Proof. There is an inclusion of B' into the 3-manifold $N(B')$, which is a homotopy equivalence. Hence, associated with the kernel of $\mu\colon \pi_1(B') \to O(2)$, there is a covering space of $N(B')$, which we denote by $N(\tilde{B})$. This is a regular neighbourhood of $\tilde{B}$ and hence is the required 3-manifold. Note that there is a collapsing map $\pi\colon N(\tilde{B}) \to \tilde{B}$. □

PROPERTY 9.4. *$\tilde{B}$ has trivial monodromy.*

Proof. Implicit in this statement is the assertion that one can define a monodromy homomorphism $\tilde{\mu}\colon \pi_1(\tilde{B}) \to O(2)$. But the method of doing this is by direct analogy with the case of B'. By construction, the monodromy homomorphism of $\tilde{B}$ has trivial image. □

PROPERTY 9.5. *$\tilde{B}$ is transversely orientable.*

Proof. The obstruction to finding a transverse orientation to a branched surface is the existence of a closed loop ℓ in the branched surface, so that as one travels around this loop and keeps track of a transverse orientation, this is reversed by the time one returns to the starting point. This is evident in the

monodromy homomorphism $\tilde{\mu}$. For then $\tilde{\mu}(\ell)$ has nontrivial image after composing with the determinant homomorphism $O(2) \to \{\pm 1\}$. This contradicts the fact that $\tilde{\mu}$ has trivial image. □

PROPERTY 9.6. *The number of Euclidean patches of $\tilde{B}$ is at most $192n^2$.*

Proof. This follows from the fact that the number of Euclidean patches of B is at most $24n^2$. □

PROPERTY 9.7. *The total length of the intersection between the singular locus of $\tilde{B}$ and the Euclidean patches of $\tilde{B}$ is at most $768n^2$.*

Proof. The singular locus is a subset of the 1-skeleton of $\tilde{B}$. Since each Euclidean patch of $\tilde{B}$ is isometric to a Euclidean square of side length 1, the total length of the singular locus incident to the Euclidean patches is at most four times the number of Euclidean patches. □

There is an inclusion $i\colon \hat{E} \to N(B')$ and a collapsing map $\pi\colon N(B') \to B'$. The kernel of $\mu\pi_* i_*$ is a finite index subgroup of $\pi_1(\hat{E})$. Let $\tilde{E}$ be the corresponding covering space of $\hat{E}$. Then $\tilde{E}$ is carried by $\tilde{B}$.

The actual result we will prove in this section is as follows.

PROPOSITION 9.8. *Suppose that there is a point x in $\tilde{E}$ with distance more than $8000n^2$ from $\partial\tilde{E}$. Then $\tilde{E}$ has a torus summand, when viewed as a surface carried by the branched surface $\tilde{B}$.*

We now show how Theorem 7.3 follows from this.

We are supposing that there is a point z in E' with distance more than $8000n^2$ from ∂E. Let $\tilde{z}$ be a point in the inverse image of z in $\tilde{E}$. Then this has distance more than $8000n^2$ from $\partial\tilde{E}$. This is because a path from $\tilde{z}$ to $\partial\tilde{E}$ projects to a path from z to ∂E with the same length. So, applying Proposition 9.8, we deduce that $\tilde{E}$ has a torus summand T.

Now, the covering map $\tilde{B} \to B'$ sends $[\tilde{E}]$ to a nonzero multiple $m[\hat{E}]$ of $[\hat{E}]$. The covering map sends $[T]$ to a vector satisfying the matching equations for B' and with zero boundary. This corresponds to a closed surface T' carried by B'. By Lemma 8.2, T' is a summand of $m[\hat{E}]$. Since T' is a closed surface, Lemmas 8.3 and 9.2 imply that T' is also carried by B_S. So, $[T']$ is a summand of $m[S]$. We deduce that S is not a boundary-vertex surface. But this is contrary to the hypothesis of Theorem 7.3.

Thus, Proposition 9.8 implies Theorem 7.3. We therefore now work almost exclusively with $\tilde{E}$ and $\tilde{B}$. We fix a transverse orientation of $\tilde{B}$. This induces a transverse orientation of $\tilde{E}$.

9.4. *Grids and annuli.* The proof now divides into two cases. Either there is a closed geodesic in $\tilde{E} - N_{1000n^2}(\partial\tilde{E})$ with length at most $12000n^2$, or there is not.

Suppose first that there is such a closed geodesic. Since $\tilde{E}$ has trivial monodromy, this closed geodesic is a multiple of a simple closed geodesic α.

Now, α represents a nontrivial element of $\pi_1(\tilde{E})$. Let $\tilde{E}_\infty$ be the universal cover of $\tilde{E}$, and let $\tilde{\alpha}$ be one component of the inverse image of α in $\tilde{E}_\infty$. Then corresponding to α, there is a covering transformation τ of $\tilde{E}_\infty$. For each point $\tilde{x}_\infty$ on $\tilde{\alpha}$, τ acts on $\tilde{x}_\infty$ by translation along $\tilde{\alpha}$. This is also true of points close to $\tilde{x}_\infty$. Now if $N_r(\tilde{\alpha})$ is disjoint from $\partial\tilde{E}_\infty$, for some $r > 0$, then $N_r(\tilde{\alpha})$ is isometric to $[-r, r] \times \tilde{\alpha}$. Hence, $N_r(\tilde{\alpha})/\langle\tau\rangle$ is isometric to $[-r, r] \times \alpha$. The covering map $\tilde{E}_\infty \to \tilde{E}$ sends $N_r(\tilde{\alpha})$ onto $N_r(\alpha)$. If there are two points of $N_r(\tilde{\alpha})$ that do not differ by an element of $\langle\tau\rangle$ but that are sent to the same point in $N_r(\alpha)$, then $\tilde{E}$ is a torus. This is impossible because $\partial\tilde{E}$ is nonempty. We therefore deduce that $N_r(\alpha)$ is isometric to a Euclidean annulus. Summarising, we have proved the following.

LEMMA 9.9. *Suppose that α is a simple closed geodesic in $\tilde{E} - N_{1000n^2}(\partial\tilde{E})$ with length at most $12000n^2$. Then, for all $r \leq 1000n^2$, $N_r(\alpha)$ is a Euclidean annulus with core curve α.*

Suppose now there is no closed geodesic in $\tilde{E} - N_{1000n^2}(\partial\tilde{E})$ with length at most $12000n^2$. Then, the exponential map based at any $x \in \tilde{E} - N_{7000n^2}(\partial\tilde{E})$ defines an isometry between a Euclidean disc of radius $6000n^2$ and $N_{6000n^2}(x)$. Let x lie at the centre of a tile. Hence, centred at x, there is a *grid*, which is a union of square tiles that is isometric to Euclidean square. (See Figure 28.) We may find such grids with any odd integer side length less than $6000\sqrt{2}n^2$. Note that $8000n^2 + 1 \leq 6000\sqrt{2}n^2$.

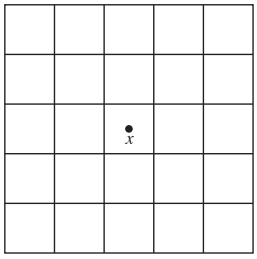

Figure 28. A grid centred at x

For a positive integer $r \leq 4000n^2$ and any $x \in \tilde{E} - N_{7000n^2}(\partial\tilde{E})$, we let $D(x, r)$ denote a grid centred at a tile containing x with side length $2r + 1$. Note that when x lies in more than one tile, this is slightly ambiguous, but this ambiguity will not cause any problems.

The proof now divides into these two cases. We focus first on the case where each x in $\tilde{E} - N_{7000n^2}(\partial\tilde{E})$ lies in the central tile of a grid with side length $8000n^2 + 1$.

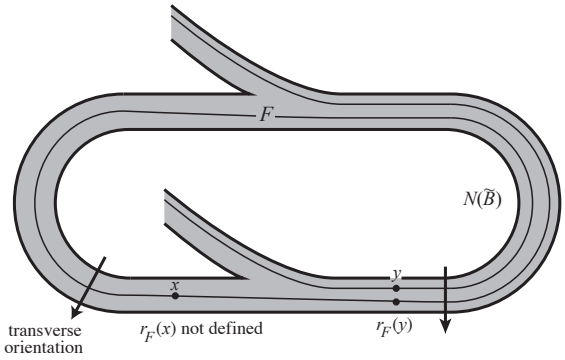

Figure 29. First-return map

9.5. *First-return maps.* For a transversely oriented subsurface F of $\tilde{E}$, we now define the *first-return map*. This is function (which need not be continuous) $r_F \colon \mathrm{dom}(r_F) \to F$, where the domain of definition $\mathrm{dom}(r_F)$ is a subsurface of F. For each point x in F, there is a fibre I_x in $N(\tilde{B})$ through x. This fibre is divided into two by x. Let α_x be the component of $I_x - \{x\}$ into which F points at x. Define $\mathrm{dom}(r_F)$ to be those $x \in F$ such that $\alpha_x \cap F \neq \emptyset$. For $x \in \mathrm{dom}(r_F)$, define $r_F(x)$ to be the point of $\alpha_x \cap F$ that is closest to x in α_x.

LEMMA 9.10. *If $F \subseteq F'$, then $\mathrm{dom}(r_F) \subseteq \mathrm{dom}(r_{F'})$.*

Proof. If $x \in \mathrm{dom}(r_F)$, then $\alpha_x \cap F \neq \emptyset$, and so $\alpha_x \cap F' \neq \emptyset$. Therefore $x \in \mathrm{dom}(r_{F'})$. □

LEMMA 9.11. *r_F does not have a fixed point.*

Proof. This is because, for each $x \in \mathrm{dom}(r_F)$, x and $r_F(x)$ are distinct points in the fibre I_x. □

LEMMA 9.12. *If F is a connected subsurface of $\tilde{E}$ that is a union of Euclidean tiles, then $F - \mathrm{dom}(r_F)$ consists of at most $192n^2$ tiles.*

Proof. For each Euclidean patch of $\tilde{B}$, the tiles of F in the fibred neighbourhood of this patch are parallel. Since F is connected and $\tilde{B}$ is transversely orientable, these tiles of F are all coherently oriented. Hence, on all but one of these tiles of F, r_F is defined. There are at most $192n^2$ Euclidean patches of $\tilde{B}$, by Property 9.6, which establishes the lemma. □

9.6. *The first-return map for large grids.* The following is an easy observation.

LEMMA 9.13. *Let D be a grid with side length at least $14n$. Then r_D is defined at some point of D.*

Proof. The branched surface $\tilde{B}$ contains at most $192n^2$ patches. Since D has at least $196n^2$ tiles, D must run over some patch of $\tilde{B}$ at least twice. Hence, r_D is defined on one of these patches in D. □

However, we need the following rather stronger statement.

PROPOSITION 9.14. *Every point $x \in \tilde{E} - N_{7000n^2}(\partial\tilde{E})$ lies in the domain of definition of $r_{D(x,4000n^2)}$.*

The key step in the proof of this is the assertion that, for a large grid D, the points in D where $r_{\tilde{E}}$ fails to be defined lie close to ∂D. In fact, it is convenient to work with several grids simultaneously, as follows.

PROPOSITION 9.15. *Let $D_1, \ldots, D_m \subseteq \tilde{E}$ be a collection of disjoint grids, each with side length at least $1500n^2$. For each D_i, let d_i be $\sup\{d(y, \partial D_i) : y \in D_i - \mathrm{dom}(r_{\tilde{E}})\}$. Then $\sum_i d_i \leq 384n^2$.*

Proof. Let D denote the union of the grids $D_1, \ldots, D_m$. We now form a union of annuli and discs C in $N(\tilde{B})$, such that $\tilde{E} \cap C \subseteq \partial C$, as follows. Start with the cusps of $N(\tilde{B})$. In a regular neighbourhood of the Euclidean patches of $\tilde{B}$, the cusps of $\tilde{B}$ are annuli and discs. This follows from Lemma 8.1, setting M to be this regular neighbourhood of the Euclidean patches and considering the branched surface $\tilde{B} \cap M$. Hence, we may extend each such cusp vertically into the interior of $N(\tilde{B})$ until it just touches $\tilde{E}$. (See Figure 30.) Let C be the result. Note that $C \cap \tilde{E}$ is a collection of simple closed curves and properly embedded arcs in $\tilde{E}$. Divide $C \cap \tilde{E}$ into $\partial_- C$ and $\partial_+ C$, where the transverse orientation on $\tilde{E}$ points into C at $\partial_- C$, and out of C at $\partial_+ C$. Then $\partial_- C \cap D$ forms the intersection between $D \cap \mathrm{dom}(r_{\tilde{E}})$ and $\mathrm{cl}(D - \mathrm{dom}(r_{\tilde{E}}))$. It is a collection of simple closed curves and properly embedded arcs in D.

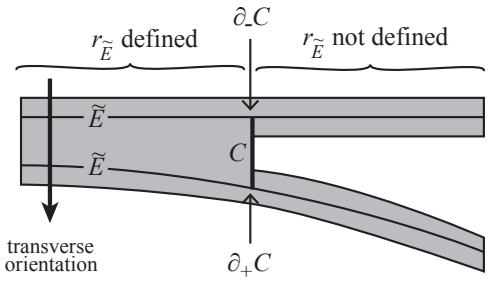

Figure 30. The annuli C

CLAIM 1. *For each grid D_i, any point on $\partial_- C \cap D_i$ that is furthest from ∂D_i lies on an arc component of $\partial_- C \cap D_i$.*

Let us assume the claim for the moment. Now, the total length of the cusps of $\tilde{B}$ is at most $768n^2$, by Property 9.7, and so $\partial_- C \cap D$ also has length at most $768n^2$. Consider a point p on $\partial_- C \cap D_i$ that has maximal distance from ∂D_i. By the claim, p can be at a distance at most $384n^2$ from ∂D_i. Let D_i' be the grid with the same centre as D_i, but with p on its boundary. Hence, the interior of D_i' either lies entirely in $\mathrm{dom}(r_{\tilde{E}})$ or is entirely disjoint from $\mathrm{dom}(r_{\tilde{E}})$. But, by Lemma 9.12, $\mathrm{dom}(r_{\tilde{E}})$ is defined for all but at most $192n^2$ tiles. We are assuming that D_i has side length at least $1500n^2$. Hence, the side length of D_i' is at least $1500n^2 - (2 \times 384n^2) = 732n^2$. Therefore there are at least $(732n^2)^2$ tiles in D_i', which is more than $192n^2$. So, we deduce that D_i' lies in $\mathrm{dom}(r_{\tilde{E}})$. Therefore, a point in $\mathrm{cl}(D_i - \mathrm{dom}(r_{\tilde{E}}))$ at maximal distance from ∂D_i must lie in $\partial_- C \cap D_i$. So, d_i is at most half the length of $\partial_- C \cap D_i$. Therefore, $\sum d_i$ is at most half the length of $\partial_- C \cap D$, which is at most $384n^2$. This proves the proposition.

We still need to prove Claim 1.

We give $\partial_- C \cap D$ a transverse orientation in D, pointing it towards $\mathrm{dom}(r_{\tilde{E}})$. Thus, it points 'into' $\tilde{B}$ and away from the cusps.

Claim 2. *Each simple closed curve of $\partial_- C \cap D$ points into the disc in D that it bounds.*

Claim 1 is a consequence of Claim 2, as follows. Cut D_i along the arc components of $\partial_- C \cap D_i$, and let D_i'' be the disc containing the centre of D_i. Since the arc components have length at most $768n^2$, D_i'' contains the grid with the same centre as D_i and with side length $732n^2 - 1$. So, D_i'' contains at least $(732n^2 - 1)^2$ tiles. We will rule out the possibility that there are any simple closed curves of $\partial_- C$ in D_i''. Let γ be the union of those components of $\partial_- C \cap \mathrm{int}(D_i'')$ that are outermost, in other words, that do not lie within another component of $\partial_- C \cap \mathrm{int}(D_i'')$. The total length of γ is at most $768n^2$, and so the total number of tiles that it can bound is at most $(768n^2)^2/4 = (384n^2)^2$. But by Claim 2, $\mathrm{dom}(r_{\tilde{E}}) \cap D_i''$ lies within γ. So, at least $(732n^2 - 1)^2 - (384n^2)^2$ tiles do not lie in $\mathrm{dom}(r_{\tilde{E}})$. However, we have already seen in Lemma 9.12 that $r_{\tilde{E}}$ is defined on all but at most $192n^2$ tiles of $\tilde{E}$. This is a contradiction, proving Claim 1.

We now must prove Claim 2. Suppose that there is a simple closed curve component β of $\partial_- C \cap D$ that points out of the disc that it bounds in D. We therefore get a configuration as shown in Figure 31.

Let $\tilde{C}'$ be the component of C containing β. Let C' be the image of $\tilde{C}'$ in $N(B')$ under the covering map $N(\tilde{B}) \to N(B')$. This is a cusp of $N(B')$ that has been extended to E'. Let $2S$ be two normally parallel copies of the characteristic surface S. Shrink the annulus C' a little so that its boundary lies in $2S$. Let C'' be the resulting annulus. It is embedded. (Note that C'

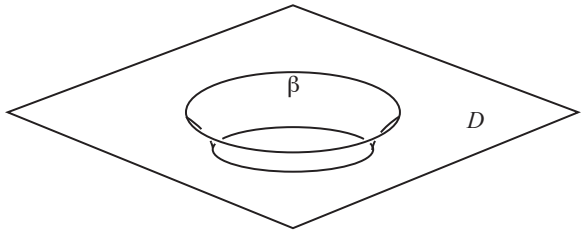

Figure 31. An outward-pointing cusp

might not have been embedded since its two boundary components might have intersected each other.) The two curves $\partial C''$ bound discs W_1 and W_2 in $2S$. One of these discs is parallel to the image in E' of the disc in D bounded by β. Hence, W_1 and W_2 are not normally parallel, because the cusp C'' lies between them.

Now, W_1 and W_2 are disjoint. For if they were nested, say $W_1 \subset W_2$, then we could remove W_2 from S and replace it by W_1, thereby creating a normal characteristic surface S' with the same boundary as S, but with $(w_\beta(S'), w(S')) < (w_\beta(S), w(S))$.

We now form two new normal characteristic surfaces S_1 and S_2 with the same boundary as $2S$. The first of these is obtained from $2S$ by removing W_2 and replacing it with a normally parallel copy of W_1. Similarly, S_2 is obtained from $2S$ by removing W_1 and inserting a normally parallel copy of W_2. Then S_1 and S_2 are both distinct from $2S$, up to normal isotopy, because W_1 and W_2 are not normally parallel. Note that, as normal surfaces, $4S = S_1 + S_2$. Hence, we deduce that S is not a boundary-vertex surface. This contradiction proves Claim 2. □

Proof of Proposition 9.14. Let x be a point in $\tilde{E} - N_{7000n^2}(\partial\tilde{E})$. We will define two increasing sequences of nonnegative integers m_i and k_i and a collection of maps $D(x, 2000n^2 - k_i) \times [0, m_i] \to N(\tilde{B})$ with the following properties:

(1) the map is an embedding on $D(x, 2000n^2 - k_i) \times [0, m_i)$;
(2) $D(x, 2000n^2 - k_i) \times \{0\} = D(x, 2000n^2 - k_i) \subset \tilde{E}$;
(3) the transverse orientation on $D(x, 2000n^2 - k_i)$, which is inherited from that of $\tilde{E}$, points into $D(x, 2000n^2 - k_i) \times [0, m_i)$;
(4) for each point $\{*\}$ in $D(x, 2000n^2 - k_i)$, $\{*\} \times [0, m_i]$ is a subset of a fibre in $N(\tilde{B})$;
(5) $(D(x, 2000n^2 - k_i) \times [0, m_i]) \cap \tilde{E} = D(x, 2000n^2 - k_i) \times ([0, m_i] \cap \mathbb{Z})$.

This sequence will continue until $D(x, 2000n^2 - k_i) \times \{m_i\} \subseteq \tilde{E}$ has nonempty intersection with $D(x, 2000n^2) \subseteq \tilde{E}$.

We start with $D(x, 2000n^2) \times \{0\}$. Set i, m_0 and k_0 to be 0. We now apply the following procedure:

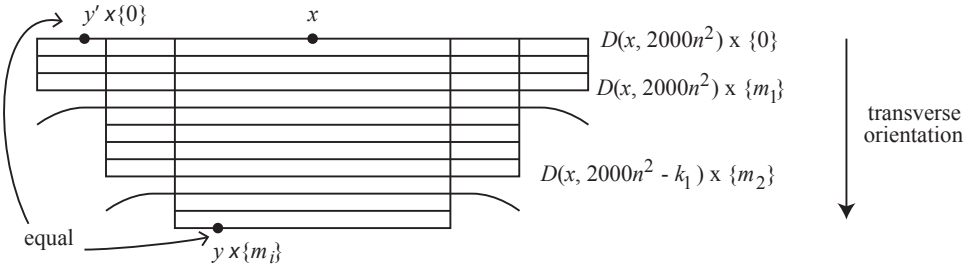

Figure 32. Schematic picture of the product regions

(1) Suppose $D(x, 2000n^2 - k_i) \times [0, m_i]$ has been defined and that $m_i > 0$. If $D(x, 2000n^2 - k_i) \times \{m_i\}$ is disjoint from $D(x, 2000n^2)$, then add it to this product region. Increase m_i by 1. Pass to step (2). If $D(x, 2000n^2 - k_i) \times \{m_i\}$ intersects $D(x, 2000n^2)$, then the procedure terminates.

(2) Is $r_{\tilde{E}}(y)$ defined for all $y \in D(x, 2000n^2 - k_i) \times \{m_i\}$? If not, then pass to step (3). Otherwise, remain on this step. This means that below $D(x, 2000n^2 - k_i) \times \{m_i\}$, there is another part of $\tilde{E}$. Define this to be $D(x, 2000n^2 - k_i) \times \{m_i + 1\}$. Between these two surfaces, there is a product region, which we take to be $D(x, 2000n^2 - k_i) \times (m_i, m_i + 1)$. Return to step (1).

(3) In this situation, $r_{\tilde{E}}(y)$ is not defined for some $y \in D(x, 2000n^2 - k_i) \times \{m_i\}$. This means that there is at least one cusp of $N(\tilde{B})$ directly below some part of $D(x, 2000n^2 - k_i) \times \{m_i\}$. Let d_i be the maximal distance of such a cusp from the boundary of $D(x, 2000n^2 - k_i) \times \{m_i\}$. Applying Proposition 9.15 to the discs $D(x, 2000n^2 - k_0) \times \{m_0\}, \dots, D(x, 2000n^2 - k_i) \times \{m_i\}$ gives that $\sum_{j=1}^{i} d_j$ is at most $384n^2$. Set $k_{i+1} = \sum_{j=1}^{i} d_j$. Therefore $D(x, 2000n^2 - k_{i+1})$ is a grid of side length at least $2 \times (2000n^2 - 384n^2) \geq 1500n^2$. Let $m_{i+1} = m_i + 1$. Increase i by 1, and pass to step (1).

When this process terminates, we deduce the existence of points $y \in D(x, 2000n^2 - k_i)$ and $y' \in D(x, 2000n^2)$ such that $y \times \{m_i\} = y' \times \{0\}$. Thus, $r_{D(x,2000n^2)}(y) = y'$.

We now extend $D(x, 2000n^2)$ to the grid $D(x, 4000n^2)$. Now, $x \times \{m_i\}$ lies within the grid $D(y \times \{m_i\}, 2000n^2)$. Hence, we deduce that $x \times \{m_i\}$ lies in $D(x, 4000n^2)$. There may be other points of $D(x, 4000n^2)$ on the fibre between $x \times \{0\}$ and $x \times \{m_i\}$. But we deduce that the first-return map for $D(x, 4000n^2)$ is defined at x. □

9.7. *Translation invariance of first-return maps.* Let x be a point in $\tilde{E} - N_{7000n^2}(\partial \tilde{E})$. The points x and $r_{D(x,4000n^2)}(x)$ both lie in the disc $D(x, 4000n^2)$ and so there is a well-defined Euclidean translation vector v_x taking x to $r_{D(x,4000n^2)}(x)$. This vector lies in the tangent space $T_x\tilde{E}$.

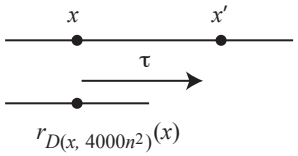

Figure 33. Translating x to x'

PROPOSITION 9.16. *The vector field* $\{v_x : x \in \tilde{E} - N_{7000n^2}(\partial\tilde{E})\}$ *is covariant constant.*

In other words, this vector field on a component of $\tilde{E} - N_{7000n^2}(\partial\tilde{E})$ is the same as the one obtained by starting with the vector v_x for some fixed x in that component and translating using Euclidean parallel translation.

Proof. Clearly the vector field is covariant constant on each tile, since $\tilde{B}$ has trivial monodromy. So suppose that x and x' lie at the centres of adjacent tiles t and t' of $\tilde{E}$. Let τ be the Euclidean translation of length 1 taking x to x'. Then, when passing from $D(x, 4000n^2)$ to $D(x', 4000n^2)$, the translation τ is performed. Since $\tilde{B}$ has trivial monodromy, the tile containing $r_{D(x,4000n^2)}(x)$ is also translated by τ. Hence, it lies in the same patch of $N(\tilde{B})$ as t'. We claim that this is the tile containing $r_{D(x',4000n^2)}(x')$. For otherwise, there is a tile of $D(x', 4000n^2)$ lying between it and x'. But, then translating this tile by τ^{-1}, we get a tile of $D(x, 4000n^2)$ lying between x and $r_{D(x,4000n^2)}(x)$, which is impossible. See Figure 33. □

COROLLARY 9.17. *Let* x *be a point in* $\tilde{E} - N_{7000n^2}(\partial\tilde{E})$. *Let* β *be a path starting at* x *and remaining in* $\tilde{E} - N_{7000n^2}(\partial\tilde{E})$. *Let* β' *be obtained from* β *by translating each point in the direction* v_x. *Then* $\pi \circ \beta = \pi \circ \beta'$, *where* $\pi\colon N(\tilde{B}) \to \tilde{B}$ *is the projection map.*

In other words, β and β' follow the same itinerary through $\tilde{B}$. This will be important for us, because curves of this form will become two sides of a parallelogram that will glue up to form the torus that we are looking for.

9.8. *Completion of the proof.* We are assuming that there is a point x in $\tilde{E}$ with distance more than $8000n^2$ from $\partial\tilde{E}$.

Let α be the geodesic in $D(x, 4000n^2)$ from x to $x' = r_{D(x,4000n^2)}(x)$. Let β be a geodesic going through x orthogonal to α with length $1000n^2$ in both directions from x. Then β remains in $\tilde{E} - N_{7000n^2}(\partial\tilde{E})$. Let β' be the result of translating β using the vector v_x, so that it runs through x'. Then we refer to the region between β and β' as a *strip*, and we denote it by P. It is a Euclidean rectangle.

In Section 9.4, the proof divided into two cases: when there is a closed geodesic in $\tilde{E} - N_{1000n^2}(\partial\tilde{E})$ with length at most $12000n^2$, and when there is

not. We initially focused on the case where there is no such geodesic, and we have defined x, α, β and P in this case. But now we want to reintegrate the two parts of the argument. So, suppose that there is such a geodesic, which we may take to be simple, and call it α. Let x be a point on α, and let β be a geodesic through x that is orthogonal to α. Suppose that it has length $1000n^2$ in both directions from x. We proved in Lemma 9.9 that $N_{1000n^2}(\alpha)$ is isometric to a Euclidean annulus with core curve α. Hence, β cuts $N_{1000n^2}(\alpha)$ into a Euclidean rectangle. We also call this a *strip* and denote it by P.

We now want to emulate the proof of Proposition 9.14, but instead of starting with a grid, we will start with this strip.

Let $p\colon P \to \beta$ be orthogonal projection. If V is a finite union of closed intervals in β, we say that $p^{-1}(V)$ is *strip-like*.

We will define an increasing sequence of nonnegative integers m_i and a collection of strip-like subsets $P = P_0 \supseteq P_1 \supseteq \cdots \supseteq P_k$ of P, with the following properties:

(1) there is map $P_i \times [0, m_i] \to N(\tilde{B})$ that is an embedding on $P_i \times [0, m_i)$;
(2) $P_i \times \{0\} = P_i \subseteq P$;
(3) the transverse orientation on P_i points into $P_i \times [0, m_i)$;
(4) for each point $\{*\}$ in P_i, $\{*\} \times [0, m_i]$ is a subset of a fibre in $N(\tilde{B})$;
(5) the intersection between $P_i \times [0, m_i]$ and $\tilde{E}$ is $P_i \times ([0, m_i] \cap \mathbb{Z})$.

This sequence will continue until $P_i \times \{m_i\} \subseteq \tilde{E}$ has nonempty intersection with $P \subseteq \tilde{E}$.

We start with $P_0 = P \times \{0\}$. Set i and m_0 to be 0. We now apply the following procedure:

(1) Suppose that $m_i > 0$, that $P_i \times [0, m_i] \to N(\tilde{B})$ has been defined and that it is an embedding on $P_i \times [0, m_i)$. If $P_i \times \{m_i\}$ is disjoint from P, then add it to this product region. Increase m_i by 1. Pass to step (2). If $P_i \times \{m_i\}$ intersects P, then terminate this procedure.
(2) Is $r_{\tilde{E}}(y)$ defined for all $y \in P_i \times \{m_i\}$? If not, then pass to step (3). Otherwise, remain on this step. This means that below $P_i \times \{m_i\}$, there is another part of P. Define this to be $P_i \times \{m_i + 1\}$. Between these two surfaces, there is a product region, which we take to be $P_i \times (m_i, m_i + 1)$. Return to step (1).
(3) In this situation, $r_{\tilde{E}}(y)$ is not defined for some $y \in P_i \times \{m_i\}$. This means that there is at least one cusp of $N(\tilde{B})$ directly below some part of $P_i \times \{m_i\}$. Extend these cusps vertically into $N(\tilde{B})$ until they just touch $P_i \times \{m_i\}$. Let C_i be the intersection of these extended cusps with $P_i \times \{m_i\}$, and let $N(C_i)$ be a thin regular neighbourhood of C_i. Define P_{i+1} to be $P_i - \mathrm{int}(p^{-1}p(N(C_i))$. This is strip-like. Let $m_{i+1} = m_i + 1$. Increase i by 1, and pass to step (1).

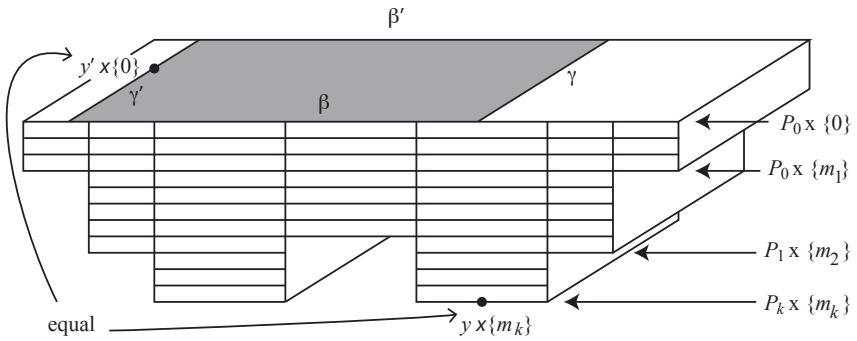

Figure 34. Schematic picture of the product regions and strip-like regions

Now, the total length of $C_1 \cup \cdots \cup C_k$ is at most $768n^2$. Therefore, the length of $p(C_1 \cup \cdots \cup C_k)$ is also at most $768n^2$. We therefore deduce that when this process terminates, P_k is nonempty. It terminates because, for some $y \in P_k$, $\{y\} \times \{m_k\}$ equals some $y' \in P \times \{0\}$. Let γ be a geodesic starting at $y \times \{0\}$ in the direction of α, and define γ' similarly starting at $y' \times \{0\}$. Then $\gamma \times [0, m_k] \subset P_k \times [0, m_k]$ forms a product region between γ and γ', where each fibre in this product region lies in a fibre in $N(\tilde{B})$. Hence, γ and γ' follow the same itinerary in $\tilde{B}$.

Let δ be the subset of β lying between $\beta \cap \gamma$ and $\beta \cap \gamma'$. Define $\delta' \subset \beta'$ similarly. Then $\gamma \cup \delta \cup \gamma' \cup \delta'$ forms the boundary of rectangle in $\tilde{E}$. Opposite sides of this rectangle have the same image in $\tilde{B}$. Hence, if we identify opposite sides of this rectangle, the result is a torus that is carried by $\tilde{B}$. It is a summand of $\tilde{E}$ by Lemma 8.2.

This proves Proposition 9.8, which completes the proof of Theorem 7.3 and hence the main results of this paper. □

10. **Final remarks**

10.1. *Improving the degree of the polynomials.* We now know that there is a polynomial upper bound on the number of Reidemeister moves required to turn a diagram of the unknot or split link into a trivial or disconnected diagram. It is natural to try to determine the smallest possible degree of such a polynomial. The result of Hass and Nowik [15] implies that one cannot do better than a quadratic polynomial. However, the degrees of the polynomials in Theorems 1.1 and 1.2 are 11.

This can certainly be reduced from 11 to 10, as follows. In the proof of Theorem 1.4, we started with a reducing 2-sphere with binding weight at most $n2^{7n^2}$, where n is the arc index. However, if one starts with a diagram of the link having c crossings, then one can find a triangulation of its exterior using at

most $8c$ tetrahedra and hence find a reducing sphere with weight at most $c2^{56c}$ with respect to this triangulation. One can then compare this triangulation with that of Dynnikov and hence find a reducing sphere with binding weight that is an exponential function of c rather than c^2. If one follows the remainder of the argument of Theorem 1.4, one finds that one has reduced the degree of the polynomial in Theorem 1.2 by 1 down to 10. One can do the same for the polynomial in Theorem 1.1. We have chosen not to pursue this argument here, because it is somewhat lengthy.

It seems very hard to reduce the degree below 10 using these arguments.

10.2. *Further problems.* This paper raises many interesting and difficult questions. We mention some these.

Is there a polynomial time algorithm to recognise the unknot? It is the author's best guess that there is not, but a proof of such a fact would be extremely hard.

Can the arguments in this paper be applied to other knot types? In particular, can one find an upper bound on the number of Reidemeister moves required to transform one diagram of a knot into another that is a polynomial function of the number of crossings in each diagram? Currently, the only known upper bound on Reidemeister moves for arbitrary knots, which is due to Coward and the author [5], is much larger than this. It is of the form of a tower of exponentials.

References

[1] I. Agol, Knot genus is NP, 2002, conference presentation. Zbl 1192.68305.

[2] D. Bennequin, Entrelacements et équations de Pfaff, in *Third Schnepfenried Geometry Conference*, *Vol.* 1 (Schnepfenried, 1982), *Astérisque* **107**, Soc. Math. France, Paris, 1983, pp. 87–161. MR 0753131. Zbl 0573.58022.

[3] J. S. Birman and E. Finkelstein, Studying surfaces via closed braids, *J. Knot Theory Ramifications* **7** (1998), 267–334. MR 1625362. Zbl 0907.57006. http://dx.doi.org/10.1142/S0218216598000176.

[4] J. S. Birman and W. W. Menasco, Studying links via closed braids. IV. Composite links and split links, *Invent. Math.* **102** (1990), 115–139. MR 1069243. Zbl 0711.57006. http://dx.doi.org/10.1007/BF01233423.

[5] A. Coward and M. Lackenby, An upper bound on Reidemeister moves, *Amer. J. Math.* **136** (2014), 1023–1066. MR 3245186. Zbl 06337019. http://dx.doi.org/10.1353/ajm.2014.0027.

[6] P. R. Cromwell, Embedding knots and links in an open book. I. Basic properties, *Topology Appl.* **64** (1995), 37–58. MR 1339757. Zbl 0845.57004. http://dx.doi.org/10.1016/0166-8641(94)00087-J.

[7] P. R. Cromwell and I. J. Nutt, Embedding knots and links in an open book. II. Bounds on arc index, *Math. Proc. Cambridge Philos. Soc.* **119** (1996), 309–319. MR 1357047. Zbl 0860.57007. http://dx.doi.org/10.1017/S0305004100074181.

[8] I. A. Dynnikov, Arc-presentations of links: monotonic simplification, *Fund. Math.* **190** (2006), 29–76. MR 2232855. Zbl 1132.57006. http://dx.doi.org/10.4064/fm190-0-3.

[9] W. Floyd and U. Oertel, Incompressible surfaces via branched surfaces, *Topology* **23** (1984), 117–125. MR 0721458. Zbl 0524.57008. http://dx.doi.org/10.1016/0040-9383(84)90031-4.

[10] O. Goldreich, *Computational Complexity. A Conceptual Perspective*, Cambridge Univ. Press, Cambridge, 2008. MR 2400985. Zbl 1154.68056. http://dx.doi.org/10.1017/CBO9780511804106.

[11] W. Haken, Theorie der Normalflächen, *Acta Math.* **105** (1961), 245–375. MR 0141106. Zbl 0100.19402. http://dx.doi.org/10.1007/BF02559591.

[12] W. Haken, Über das Homöomorphieproblem der 3-Mannigfaltigkeiten. I, *Math. Z.* **80** (1962), 89–120. MR 0160196. Zbl 0106.16605. http://dx.doi.org/10.1007/BF01162369.

[13] J. Hass and J. C. Lagarias, The number of Reidemeister moves needed for unknotting, *J. Amer. Math. Soc.* **14** (2001), 399–428. MR 1815217. Zbl 0964.57005. http://dx.doi.org/10.1090/S0894-0347-01-00358-7.

[14] J. Hass, J. C. Lagarias, and N. Pippenger, The computational complexity of knot and link problems, *J. ACM* **46** (1999), 185–211. MR 1693203. Zbl 1065.68667. http://dx.doi.org/10.1145/301970.301971.

[15] J. Hass and T. Nowik, Unknot diagrams requiring a quadratic number of Reidemeister moves to untangle, *Discrete Comput. Geom.* **44** (2010), 91–95. MR 2639820. Zbl 1191.57006. http://dx.doi.org/10.1007/s00454-009-9156-4.

[16] J. Hass, J. Snoeyink, and W. P. Thurston, The size of spanning disks for polygonal curves, *Discrete Comput. Geom.* **29** (2003), 1–17. MR 1946790. Zbl 1015.57008. http://dx.doi.org/10.1007/s00454-002-2707-6.

[17] G. Hemion, On the classification of homeomorphisms of 2-manifolds and the classification of 3-manifolds, *Acta Math.* **142** (1979), 123–155. MR 0512214. Zbl 0402.57027. http://dx.doi.org/10.1007/BF02395059.

[18] A. Henrich and L. H. Kauffman, Unknotting unknots, *Amer. Math. Monthly* **121** (2014), 379–390. MR 3193721. Zbl 06367521. http://dx.doi.org/10.4169/amer.math.monthly.121.05.379.

[19] W. Jaco and U. Oertel, An algorithm to decide if a 3-manifold is a Haken manifold, *Topology* **23** (1984), 195–209. MR 0744850. Zbl 0545.57003. http://dx.doi.org/10.1016/0040-9383(84)90039-9.

[20] W. Jaco and J. L. Tollefson, Algorithms for the complete decomposition of a closed 3-manifold, *Illinois J. Math.* **39** (1995), 358–406. MR 1339832. Zbl 0858.57018. Available at http://projecteuclid.org/euclid.ijm/1255986385.

[21] G. Kuperberg, Knottedness is in NP, modulo GRH, *Adv. Math.* **256** (2014), 493–506. MR 3177300. Zbl 06284931. http://dx.doi.org/10.1016/j.aim.2014.01.007.

[22] S. Matveev, *Algorithmic Topology and Classification of 3-Manifolds*, second ed., *Algorithms Comput. Math.* **9**, Springer-Verlag, New York, 2007. MR 2341532. Zbl 1128.57001.

[23] J. A. Storer, On minimal-node-cost planar embeddings, *Networks* **14** (1984), 181–212. MR 0741438. Zbl 0546.94033. http://dx.doi.org/10.1002/net.3230140202.

[24] A. Turing, Solvable and unsolvable problems, *Science News* **31** (1954), 723. Available at http://citeseerx.ist.psu.edu/viewdoc/download?doi=10.1.1.247.3954&rep=rep1&type=pdf.

(Received: April 10, 2013)
(Revised: May 20, 2014)

Mathematical Institute, University of Oxford, Oxford, UK
E-mail: lackenby@maths.ox.ac.uk